



MSU Graduate Theses

Summer 2018


Development of Rapid, Homogeneous Assay for Investigating Isopeptide Bond Formation Using Fluorescence Polarization/Depolarization Measurements

Samuel Patricc Kasson

Missouri State University, Kasson56@live.missouristate.edu

As with any intellectual project, the content and views expressed in this thesis may be considered objectionable by some readers. However, this student-scholar's work has been judged to have academic value by the student's thesis committee members trained in the discipline. The content and views expressed in this thesis are those of the student-scholar and are not endorsed by Missouri State University, its Graduate College, or its employees.

Follow this and additional works at: <https://bearworks.missouristate.edu/theses>

 Part of the [Analytical Chemistry Commons](#), [Biochemistry Commons](#), and the [Biotechnology Commons](#)

Recommended Citation

Kasson, Samuel Patricc, "Development of Rapid, Homogeneous Assay for Investigating Isopeptide Bond Formation Using Fluorescence Polarization/Depolarization Measurements" (2018). *MSU Graduate Theses*. 3292.

<https://bearworks.missouristate.edu/theses/3292>

This article or document was made available through BearWorks, the institutional repository of Missouri State University. The work contained in it may be protected by copyright and require permission of the copyright holder for reuse or redistribution.

For more information, please contact BearWorks@library.missouristate.edu.

**DEVELOPMENT OF RAPID, HOMOGENEOUS ASSAY FOR INVESTIGATING
ISOPEPTIDE BOND FORMATION USING FLUORESCENCE
POLARIZATION/DEPOLARIZATION MEASUREMENTS**

A Masters Thesis

Presented to

The Graduate College of

Missouri State University

In Partial Fulfillment

Of the Requirements for the Degree

Master of Science, Chemistry

By

Samuel P. Kasson

August 2018

Copyright 2018 by Samuel Patrice Kasson

**DEVELOPMENT OF RAPID, HOMOGENEOUS ASSAY FOR INVESTIGATING
ISOPEPTIDE BOND FORMATION USING FLUORESCENCE
POLARIZATION/DEPOLARIZATION MEASUREMENTS**

Chemistry

Missouri State University, August 2018

Master of Science

Samuel P. Kasson

ABSTRACT

Autocatalytic intramolecular isopeptide bonds have been found in nature in certain gram-positive bacterial pilus structures. Recently, splitting of these domains that are capable of autocatalytic intramolecular isopeptide bond formation have been applied to create stable, selective, bio-orthogonal Catcher/Tag systems. The CnaB2 domain found in the FbaB pilus structure of *Streptococcus pyogenes*, has yielded the Catcher/Tag, Protein/Peptide systems termed SpyCatcher and SpyTag. Recent study has focused on tag optimization, stability and bio-orthogonality evaluation, along with applications in bioconjugation. I have recombinantly expressed SpyCatcher and SpyTag-fused proteins in *E.coli*, and conjugated them to fluorescent probes in order for use in fluorescence polarization/depolarization study. Using this system, I have observed the dependence of SpyTag concentration on the formation of the isopeptide bond. I have also been able to track the formation of this bond in real time.

KEYWORDS: spycatcher, spytag, kinetics, fluorescence polarization, isopeptide bond

This abstract is approved as to form and content

Keiichi Yoshimatsu, PhD
Chairperson, Advisory Committee
Missouri State University

**DEVELOPMENT OF RAPID, HOMOGENEOUS ASSAY FOR INVESTIGATING
ISOPEPTIDE BOND FORMATION USING FLUORESCENCE
POLARIZATION/DEPOLARIZATION MEASUREMENTS**

By

Samuel P. Kasson

A Masters Thesis
Submitted to the Graduate College
Of Missouri State University
In Partial Fulfillment of the Requirements
For the Degree of Master of Science, Chemistry

August, 2017

Approved:

Keiichi Yoshimatsu, PhD

Adam Wanekaya, PhD

Gary Meints, PhD

Christopher Lupfer, PhD

Julie Masterson, PhD: Dean, Graduate College

In the interest of academic freedom and the principle of free speech, approval of this thesis indicates the format is acceptable and meets the academic criteria for the discipline as determined by the faculty that constitute the thesis committee. The content and views expressed in this thesis are those of the student-scholar and are not endorsed by Missouri State University, its Graduate College, or its employees.

ACKNOWLEDGEMENTS

First, I would like to thank my research advisor, Dr. Keiichi Yoshimatsu, for being a mentor supporting the learning of a large variety of scientific knowledge and techniques. Dr. Yoshimatsu was always around for any questions or concerns and always willing to discuss topics until everyone was on the same page of understanding and agreement even when I was having trouble with understanding certain topics. I would also like to thank him for being considerate and thoughtful when it comes to the balancing of other school responsibilities, and allowing time for preparation of school classes and projects. Thank you for all of your time Dr. Yoshimatsu.

Secondly, I would like to thank my thesis committee, Dr. Christopher Lupfer, Dr. Gary Meints, for their time in editing my theses, and a special thanks to Dr. Adam Wanekaya for his feedback, support, and allowing to use his lab in times of need. Our collaborator, Dr. Keykavous Parang at Chapman University was also indispensable. Linda Allen deserves a special thanks for being the heart of the department of chemistry and solving all problems that we could come across. I would also like to thank Dennis Kasson and Linda and William Rackley for their support and encouragements through my education.

I would like to acknowledge for financial support the: Chemistry Department, Graduate College, College of Natural and Applied Science, Office of Research Administration at Missouri State University, and ACS Ozark Local Section for financial support. pDEST14-SpyCatcher, pET28a-SpyTagMBP, pDEST14-SpyCatcher EQ, and pET28a SnoopTag-mEGFP-SpyTag were gifts from Mark Howarth (Addgene plasmid # 35044, 35050, 35045, and 72325). Finally, I would like to thank all my friends and classmates for their support in the last two years, in particular Leanna Patton, Quinton Wyatt, and Jacob Blankenship who were always there for me.

TABLE OF CONTENTS

INTRODUCTION	1
Affinity Tags	1
Isopeptide Bonds.....	7
SpyCatcher-SpyTag	10
Current Applications for SpyCatcher-SpyTag Systems.	13
Background Techniques.....	15
Objectives	19
 MATERIALS.....	 20
Chemicals.....	20
Kits.....	21
Plasmids	21
Enzymes.....	21
Bacteria	21
Instrumentation	21
Other Equipment.....	22
 METHODS	 23
General Methods.....	23
Procedures for General Molecular Biology	24
Procedures for DNA Handling.....	26
Procedures for Protein Handling.....	30
Fluorescence Polarization/Depolarization System Development	35
Fluorescence Polarization/Depolarization	40
 RESULTS AND DISCUSSION	 41
Protein Preparation.....	41
Fluorescence Polarization/Depolarization	56
 CONCLUSION.....	 68
 REFERENCES	 69
 APPENDICES	 73
Appendix A. Plasmid Maps	73
Appendix B. Fluorescence Polarization/Depolarization Graphs	76
Appendix C. Molar Equivalence on SDS-PAGE Using ImageJ	79

LIST OF TABLES

Table 1. IPTG OD ₆₀₀	32
Table 2. Protein purification table.	46

LIST OF FIGURES

Figure 1. Tag interactions for a variety of uses	1
Figure 2. Protein purification using metal-affinity chromatography	2
Figure 3. Maltose binding protein.....	3
Figure 4. Antibody-protein A interaction	4
Figure 5. Native chemical ligation.....	6
Figure 6. Isopeptide bonds.....	7
Figure 7. HK97 capsid	8
Figure 8. Autocatalytic intramolecular isopeptide bond formation.....	9
Figure 9. Isopeptide bond characteristics.....	12
Figure 10. Isopeptide bond apecificity and mechanical strength.....	13
Figure 11. IPTG	15
Figure 12. Autoinduction.....	16
Figure 13. Fluorescence polarization/depolarization.....	17
Figure 14. Fluorescence polarization/depolarization quantification.....	18
Figure 15. General research scheme	23
Figure 16. E.Z.N.A Kit Mini-Prep.....	28
Figure 17. Ni ²⁺ -NTA.....	33
Figure 18. Solid-phase peptide synthesis.....	37
Figure 19. SpyTag-FITC.....	38
Figure 20. Ninhydrin reaction.....	39
Figure 21. Protein preparation	41

Figure 22. Electrophoresis of pDEST14-SpyCatcher and pET28a SnoopTag-mEGFP-SpyTag on 1% agarose gel.....	42
Figure 23. Autoinduction cell growth curve	43
Figure 24. IPTG cell growth curve	44
Figure 25. SDS-PAGE of each fraction during the purification of SpyCatcher WT	45
Figure 26. Electrophoresis of pDEST14-SpyCatcher-EQ on 1% agarose gel.....	47
Figure 27. SDS-PAGE of each fraction during the purification of SpyCatcher EQ.....	48
Figure 28. SDS-PAGE of each Fraction during the purification of SnoopTag-mEGFP-SpyTag	50
Figure 29. Electrophoresis of pET28a-SpyTagMBP on 1% agarose gel.....	52
Figure 30. SDS-PAGE of each fraction during the purification of SpyTagMBP.....	53
Figure 31. SpyCatcher /SpyCatcher EQ activity gel scheme	55
Figure 32. Activity of SpyCatcher WT and SpyCatcher EQ determined on SDS-PAGE.....	55
Figure 33. Scheme of isopeptide bond formation activity measurement.....	57
Figure 34. SDS-PAGE showing SpyTagMBP, SpyCatcher-FITC derivative activity	57
Figure 35. Concentration gradient with differing concentration of SpyTagMBP using SDS-PAGE	58
Figure 36. Concentration dependence of SpyTagMBP using SDS-PAGE for comparison with mP	58
Figure 37. Concentration dependence of mP on SpyTag	60
Figure 38. Molar equivalence on SDS-PAGE using ImageJ	61
Figure 39. Band intensity ratio vs mP for different SpyTagMBP molar equivalence.....	61

Figure 40. Kinetic study.....	62
Figure 41. Kaiser test.....	63
Figure 42. SDS-PAGE SpyTag-FITC activity.....	65
Figure 43. BN-PAGE SpyTag-FITC activity	66
Figure 44. MALDI analysis	67

INTRODUCTION

Affinity Tags

Biochemical research relies on affinity agents that target proteins or molecules of interest from a large variety of other contaminants. One of the most accepted ways of doing this is through the use of affinity interactions between two molecules giving a tagging system. Systems like these can be used in a number of applications from purification, identification, and immobilization, but tend to suffer from their reversible binding nature.^{1,2,3} Due to the importance of the ability to specifically target biological molecules, it has been an attractive research topic to aid in the development of an irreversible, biorthogonal, tagging system (**Figure 1**).

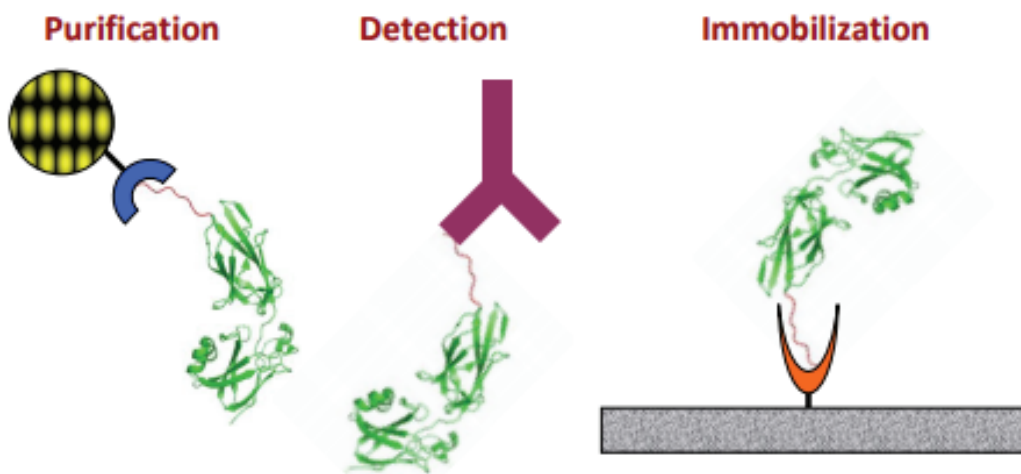


Figure 1. Tag interactions for a variety of uses. The figure shows a target protein (green) being purified, detected, or immobilized through its selective interaction with different Fab regions.⁴

Common Biological Tag Systems. One of the most widely used affinity tag system is the affinity displayed through the affinity between polyhistidine tags and metal chromatography.¹ In this system, a protein is expressed with 2-10 (commonly 6) histidine residues on one end of its sequence.¹ The imidazole rings on the histidine side chains interact strongly with metal ions and can be immobilized by them with a dissociation constant (K_d) of $5 \times 10^{-8} \text{ M}^{-1}$ (**Figure 2**).⁵ The most common use for this kind of affinity tag system is in the purification of proteins.

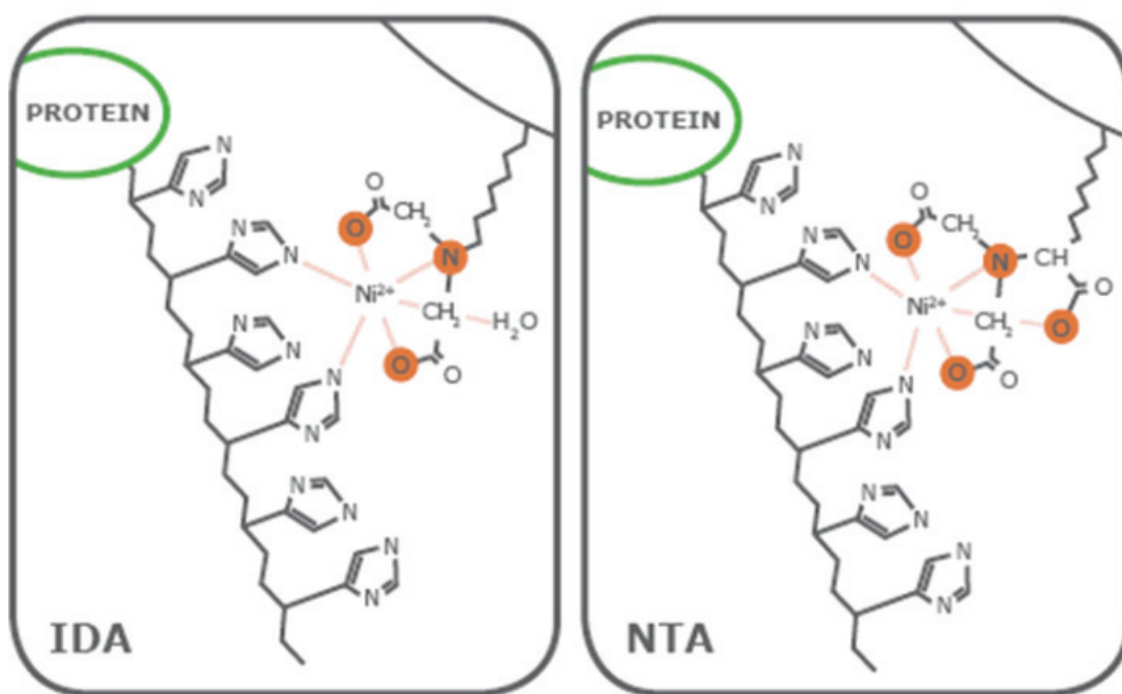


Figure 2. Protein purification using metal-affinity chromatography. Ni^{2+} -IDA (iminodiacetic acid, left) Ni^{2+} -NTA (nitrilotriacetic acid, right).⁶

Certain proteins can also be used as expression tags for use in protein purification. Glutathione s-transferase (GST) refers to a class of eukaryotic enzymes. GSTs are best known for their uses in conjugation of reduced glutathione to a number of substrates. GSTs show high binding affinity (K_d of $5 \times 10^{-8} \text{ M}^{-1}$) to glutathione which can be coupled

to a solid matrix.⁷ This tag though, in many cases, must be cleaved due to its large size (26 KDa).⁸ Maltose Binding Protein (MBP) is another example of a protein expression tag that is rather large, 42 kDa. MBP is a protein that is integral in the maltose/maltodextrin system of *Escherichia coli*.⁹ MBP shows affinity to maltose with a K_d of $2 \times 10^{-6} \text{ M}^{-1}$ and is used to purify proteins with an amylose column, unfortunately it suffers as a tag due to its large size (**Figure 3**).¹⁰

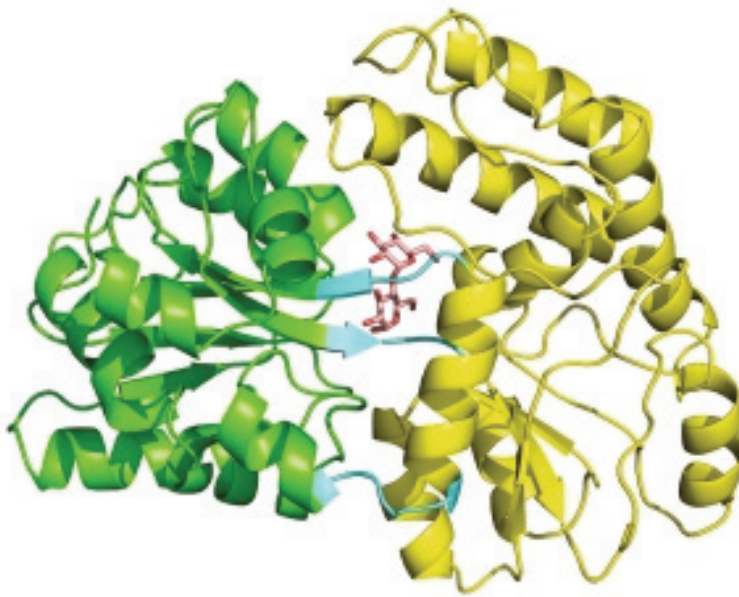


Figure 3. Maltose binding protein. Domains 1 and 2 shown in green and yellow respectively, polypeptide binding segments shown in light blue, and maltose unit shown as red © Walker, Hsieh, Riggs 2010.¹⁰

Immunoglobulin-binding proteins such as Protein A and Protein G, which are ~42 and ~65 kDa proteins respectively can be used in the affinity binding of antibodies.

Protein A was originally discovered in the cell wall of *Staphylococcus aureus* and Protein G is found in Streptococcal bacteria. Both immunoglobulin-binding proteins bind to the

fc regions of a variety of different antibodies and can be used as tags to purify proteins, or they can be immobilized to purify IgG antibodies (**Figure 4**).¹¹

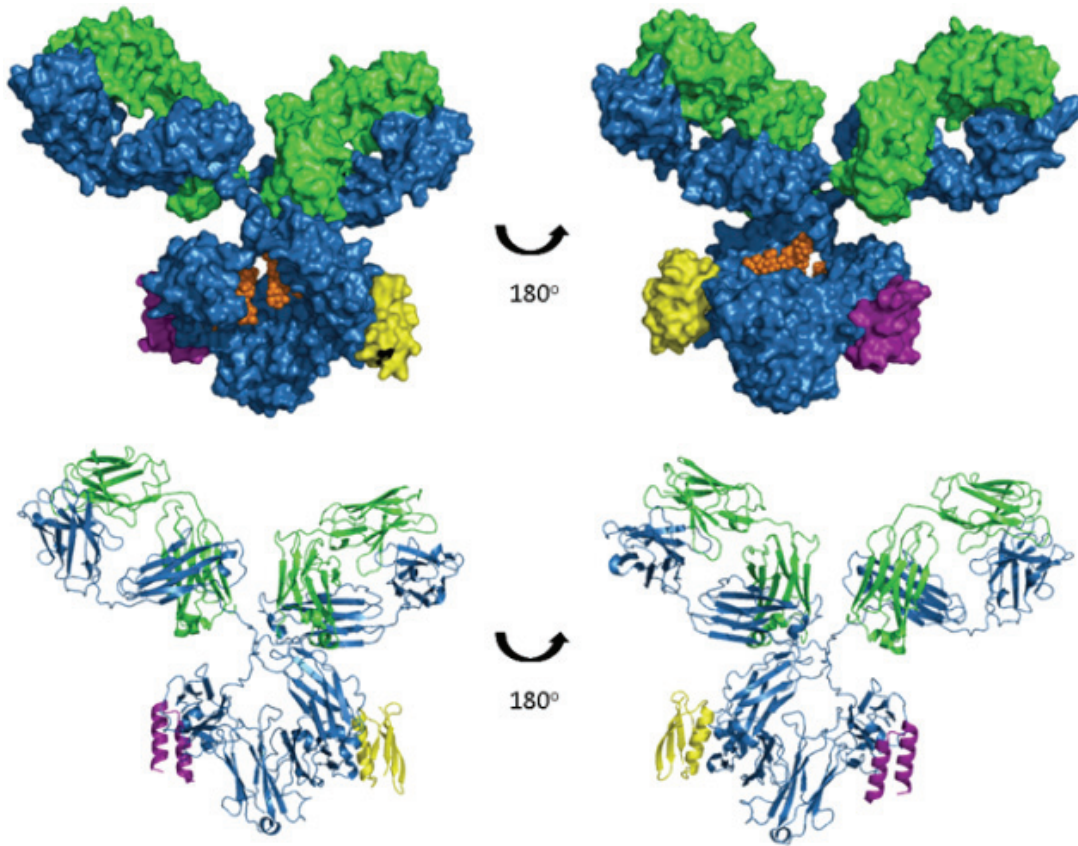


Figure 4. Antibody-protein A interaction. Space fillly model of IgG antibody (top), ribbon diagram of IgG antibody (bottom). Protein A is shown in purple, Protein G is shown in yellow. Model produced from PDB accession numbers 1IGY, 1L6X and 1FCC.¹²

Another commonly used affinity tag system is between the interaction of streptavidin and its ligand biotin (K_d $4 \times 10^{-14} \text{ M}^{-1}$). This system has one of the strongest non-covalent interactions found in nature.¹³ This system has been used in immobilization, detection, and purification steps similar to the metal affinity columns shown above.¹⁴ Through the ability to bioconjugate biotin and streptavidin to building blocks, it is

possible to assemble larger biological structures for uses such as fluorescence labeling and immunotherapy.^{15,16}

Characteristics of Affinity Tag Systems. Biological affinity tag systems must exhibit several characteristics in order to be useful tools. The first and possibly most important characteristic for catcher-tag systems is to be specific when interacting with their targets. Next, if a tag must be added to the molecule to be isolated, the tag should not affect the function of the molecule. Finally, the interactions between the catcher and tag portions of the system should be strong enough that they will not be readily broken through unintended interactions. While it is rare to find systems that display all of these characteristics, there are many biological tag systems used today that display one or more of them. Still, many of these techniques suffer from relying on non-covalent interactions between the catcher and tag resulting in relatively weak binding when compared to protein-protein interactions exploiting the use of internal cavities such as enzyme-transition state complexes.¹⁷ These systems are held through non-covalent interactions that are limited by the surface area of the binding cavity, and the limitations are likely to only be overcome through a system exploiting the formation of covalent bonds.¹⁷

Covalent Protein Linkages

Disulfide Bonds. One of the simplest ways of covalently linking peptides is through the use of disulfide bonds between the sulfur side chains of cysteine residues. Disulfide bonds can be found in many proteins as a means of inducing tertiary structure and enhancing structural stability with a bond dissociation energy of ~65 kcal/mol.¹⁸ One drawback is that there is a lack of selectivity when attempting to use disulfide bonds

because they can be transferred to nearby activated cysteine residues. This lack of selectivity can lead to large complexes and aggregations in the systems which are being linked.¹⁹ To occur, the cysteine thiol groups must be oxidized.¹⁹ In order to prevent incorrect folding, many enzymes and environments *in-vivo* do not support their formation.²⁰

Native Chemical Ligation. The use of synthetic chemistry to construct and study proteins has been a major goal in chemistry for many years. At present, the ability to construct relatively short peptides with high degrees of accuracy has been achieved, while the synthesis of longer proteins, greater than 50 amino acids, is technically difficult.²¹ In order to create a functional protein, a technique known as native chemical ligation was developed. Native chemical ligation uses the formation of a thioester intermediate which spontaneously rearranges into a peptide bond (**Figure 5**). The selectivity of this reaction hinges on the presence of an N-terminal cysteine residue. While all cysteine residues can form a thioester intermediate, only the N-terminal one may undergo the rearrangement required to irreversibly form a peptide bond.²¹

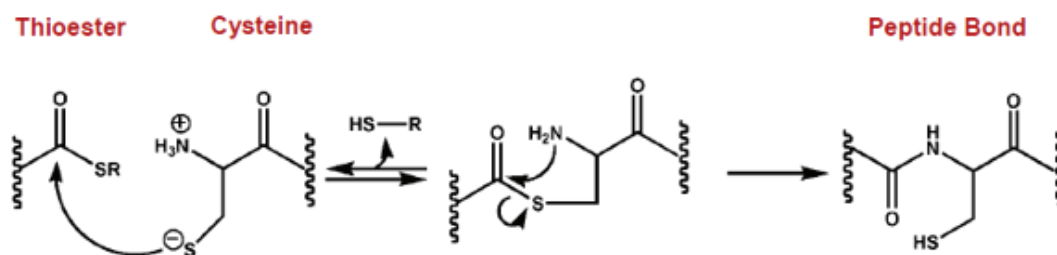


Figure 5. Native chemical ligation. Proposed mechanism for native chemical ligation.⁴

Isopeptide Bonds

Isopeptide bonds are peptide bonds that form between the side chains of a lysine and an aspartic acid, asparagine, or the C-terminal of a peptide (**Figure 6**). These bonds provide additional degrees of structure and stability to some proteins. Isopeptide bonds also hold superior bond dissociation energy (~90 kcal/mol) to many other forms of covalent bonding used in bioconjugation.¹⁸

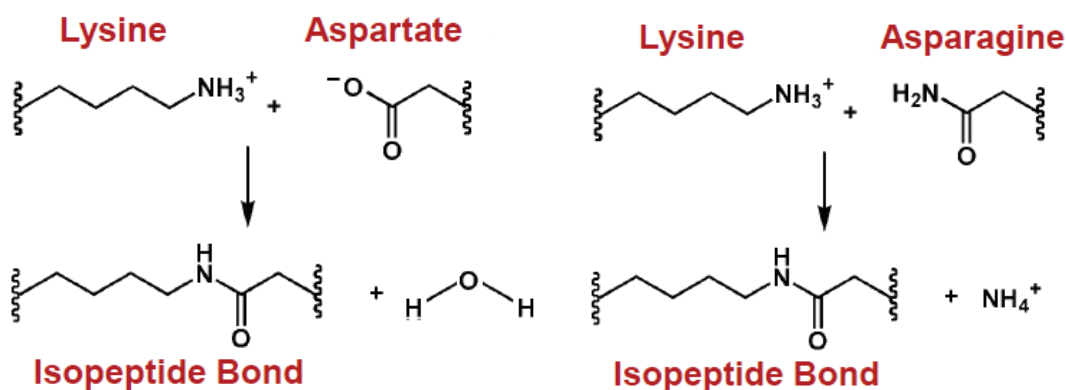


Figure 6. Isopeptide bonds. Isopeptide bond formation between an aspartic acid residue (left), or an asparagine residue (right).⁴

Intermolecular Isopeptide Bond Formation. Isopeptide bonds were first discovered as a variety of enzyme catalyzed intermolecular covalent bonds. In some organisms, a protein known as ubiquitin can attach to other proteins to mark them for degradation, relocalization, endocytosis, and in some cases can affect the proteins degree of activity through the aid of an ubiquitin enzyme complex.²² Ubiquitin function has been reported to be associated with Alzheimer's, Parkinson's, Huntingtons, and several types of cancer.^{23, 24, 25, 26} Another source of intermolecular isopeptide bonds is catalyzed by the enzyme class of transglutaminase. Transglutaminases crosslink side chains of different proteins forming isopeptide bonds increasing stability and aiding in healing.²⁷

Transglutaminases are also commonly referred to as meat glue for its use in meat processing increasing look, texture, and flavor.²⁸

The first discovery of autocatalytic isopeptide bond formation was in the HK97 bacteriophage (**Figure 7**).²⁹ In this structure, it was discovered that a proximal glutamic acid residue was catalyzing the formation of the isopeptide bond between neighboring lysine and asparagine side chains.²⁸ Through these isopeptide bonds, 420 subunits of the capsid were brought together resulting in a variable chain linking to house the viral genetic code.³⁰

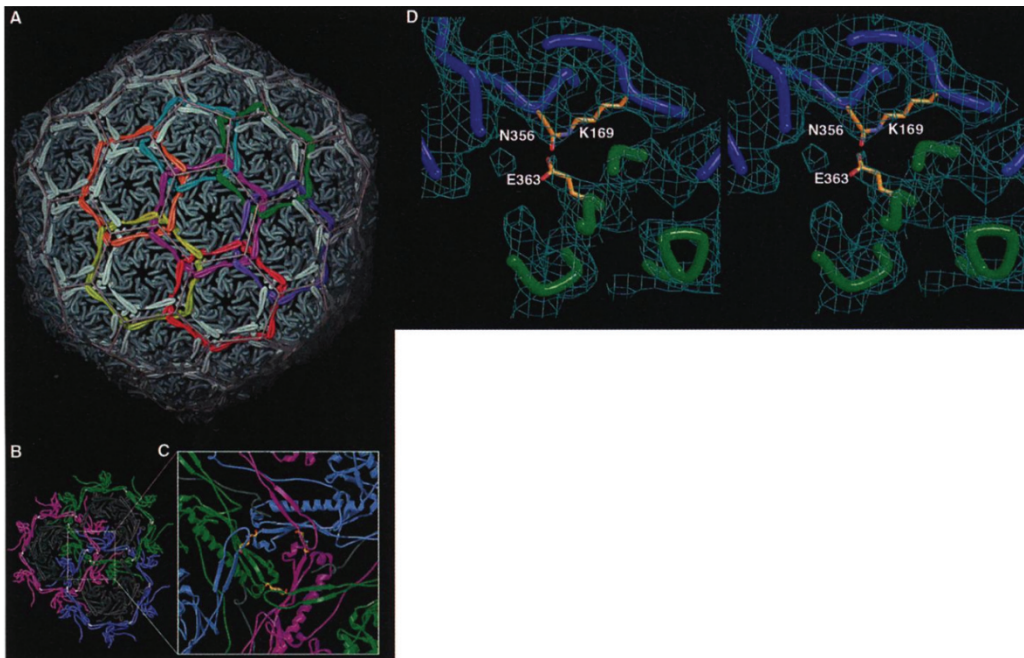
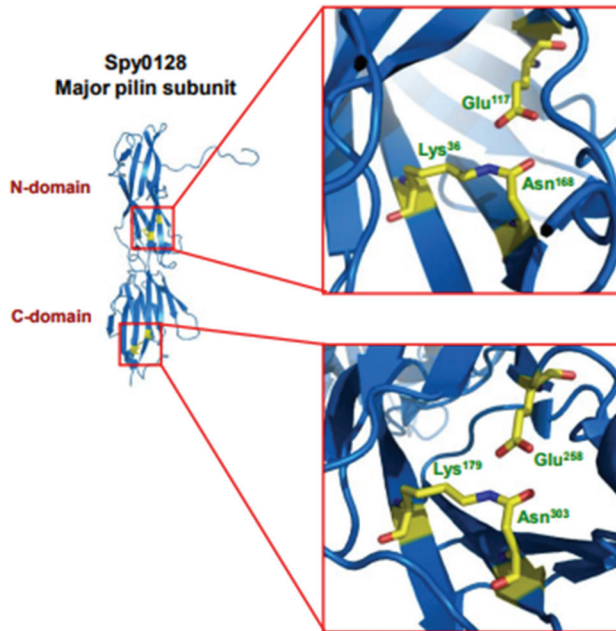


Figure 7. HK97 capsid. A: Subunits crosslinked into rings (subunits of the same ring share a color). B: View down on subunit ring interlocking. C: Enlarged view of interlocking. D: Electron density map of isopeptide bond forming area.³⁰ Copyright © 2000 The American Association for the Advancement of Science.

Intramolecular Isopeptide Bond Formation. In 2007 the first report of autocatalytic intramolecular isopeptide bonding was found in a major pilus subunit,

Spy0128, of *Streptococcus pyogenes*.³¹ The purpose of this isopeptide bond was thought to increase structural stability and resistance to mechanical, and chemical strain.³¹ These isopeptide bonds are catalyzed inside the hydrophobic cleft created in the β -sheet rich domain *via* a proximal glutamic acid residue (**Figure 8**). Since their discovery, the occurrence of isopeptide bonds in many gram positive bacterial pilus subunits including several human pathogens such as; *Staphylococcus aureus*, *Corynebacterium diphtheria*, and *Streptococcus pneumoniae*.³²

A



B

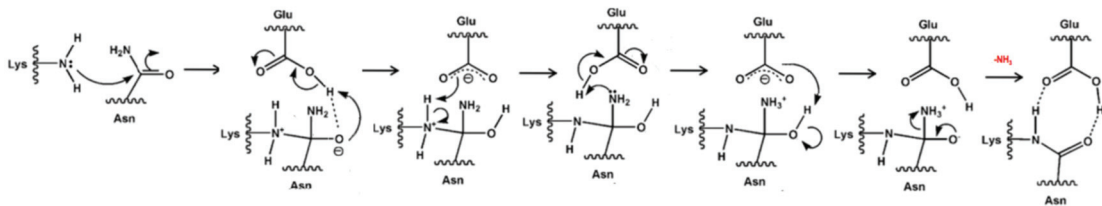


Figure 8. Autocatalytic intramolecular isopeptide bond formation. A: Major pilus subunit Spy0128 and enhanced visuals of isopeptide bond forming area.³¹ B: Proposed mechanism for autocatalytic isopeptide bond formation.⁴ Copyright © 2013 Biophysical Society. Published by Elsevier Inc.

Biological Function of Intramolecular Isopeptide Bonds in Bacteria. Many intramolecular isopeptide bonds have been discovered in the pili of bacteria. Pili are important virulence factors used by pathogenic bacteria to bind and colonize host tissues.³³ While gram-negative bacteria have evolved to stabilize their pili structures through disulfide bonds, some gram-positive bacteria have been found to utilize isopeptide bonding to stabilize and crosslink their pili subunits.³⁴ The presence of these isopeptide bonds have been shown to make these subunits resistant to trypsin digestion,³³ as well as enhancing the thermodynamic stability of these proteins increasing their melting temperature by 30 °C.³⁴ Investigations into the original autocatalytic bond forming protein Spy0128 using single molecule force spectroscopy have even shown that the protein was mechanically inextensible making it the most mechanically stable protein ever studied.³⁵

SpyCatcher-SpyTag

Recently, protein engineering on autocatalytic intramolecular isopeptide bond forming proteins has been explored. One of the first major innovations in the use of isopeptide bonding to create a protein-peptide, catcher-tag system was in the creation of the SpyCatcher-SpyTag system through the splitting of the CnaB2 domain of fibronectin binding protein (FbaB).³²

Protein Splitting. The splitting of a protein while maintaining its activity is no easy task due to the fragments needing to be maintain a level of stability while separated, and also having a high enough affinity with each other to reassemble when in proximity. Though difficult, the technique of protein splitting has been used successfully for a

variety of different proteins.³⁶ Splitting proteins has been used in several ways, one such example being in the use of super folder green fluorescent protein fragments (sfGFP) to track protein-protein interactions.³⁶ The CnaB2 domain of FbaB found in *Streptococcus pyogenes* is a β -sheet rich domain.⁴ After cleavage and specific trimming, a 13 amino acid peptide, SpyTag, containing the reactive Asp residue was formed. SpyCatcher, the 116 amino acid partner of SpyTag, contains the reactive Lys, catalytic Glu, and hydrophobic cleft needed for isopeptide bond formation.⁴

Characteristics of SpyCatcher-SpyTag System. Upon splitting of this protein domain, it was demonstrated that, when in solution, SpyCatcher and SpyTag could come together rapidly and spontaneously to form its isopeptide bonds. Due to the novel ability of this short peptide tag and protein partner to specifically and irreversibly bond to one another, more research was done into the systems stability in different environments. Isopeptide bond formation between SpyCatcher and SpyTag was only minorly affected through temperature, pH, certain detergents, and different salts (**Figure 9**).³¹

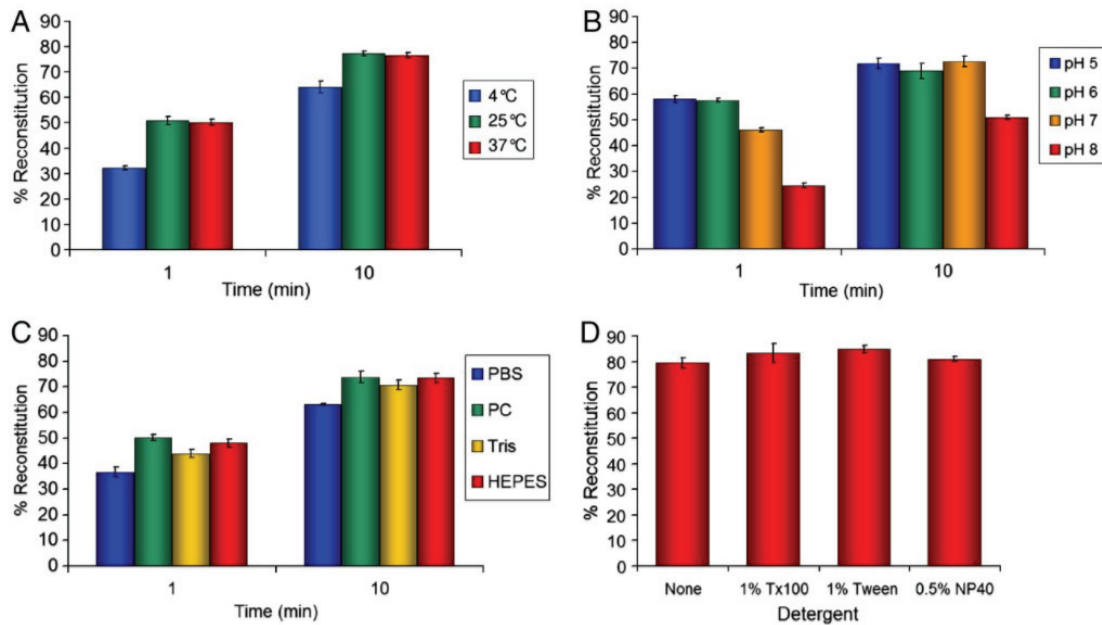


Figure 9. Isopeptide bond characteristics. Isopeptide bond formation between SpyTag-MBP and SpyCatcher at 25° C, 10 μ M, pH 7 with one variable changing. A: Temperatures, B: pHs, C: Buffers, and D: Incubated in the presence of 0detergents for 3 hours.³¹ Copyright © 2013 Biophysical Society. Published by Elsevier Inc.

Through the use of fluorescence microscopy, fluorescently labeled SpyCatcher has been seen specifically locating itself to cells expressing SpyTag fused membrane proteins demonstrating the specific interactions between these two engineered protein fragments even when in living systems. Mechanical strength was also observed to be well above what is observed in common biological targeting systems through the use of atomic force microscopy employing the I27 domain of human titin for its characteristic unfolding fingerprint (**Figure 10**).³¹

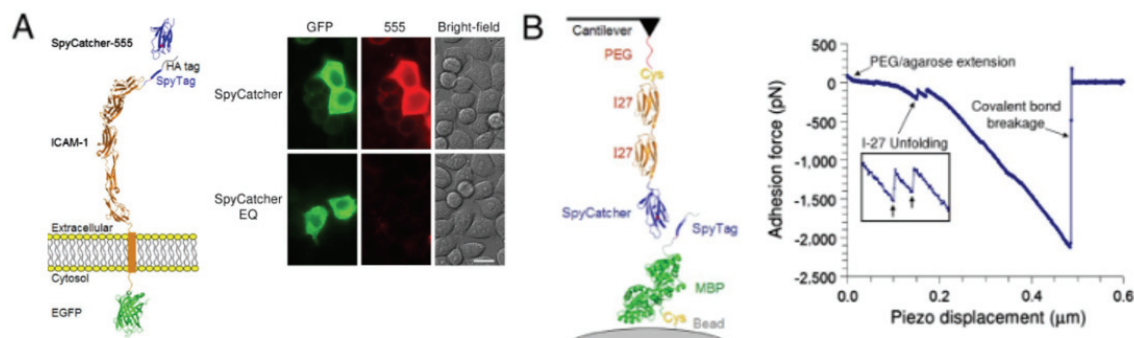


Figure 10. Isopeptide bond specificity and mechanical strength. A shows SpyCatcher labeled with Alexa-555 specifically localizing to cells expressing SpyTag-ICAM(Intercellular adhesion molecule-1)-EGFP proteins while SpyCatcher EQ (an inactive version of SpyCatcher whose catalytic Glu has been mutated to a Gln) shows no specific localization. B demonstrates a mechanical strength test performed using an atomic force microscope.³¹ Copyright © 2013 Biophysical Society. Published by Elsevier Inc.

Current Applications for SpyCatcher-SpyTag Systems.

The SpyCatcher-SpyTag system has begun being modified and used in a number of different ways including protein ligation, bioconjugation, and protein stabilization.

Functional SpyCatcher and SpyTag system derivatives. Several advancements in isopeptide forming technologies have come from the slight modifications of SpyCatcher and SpyTag such as the formation of the SpyLigase-SpyTag-KTag and SpyCatcher002-SpyTag002 systems.³⁷ The SpyLigase-SpyTag-KTag system operates in a manner similar to the SpyCatcher-SpyTag system, only the Lysine containing β -sheet found within SpyCatcher has been cleaved resulting in another short tag sequence termed KTag.³⁷ SpyLigase is the remnant of the SpyCatcher protein after this cleavage which still contains the catalytic glutamic acid residue and hydrophobic cleft that is needed for the isopeptide bond to be formed.³⁷ The SpyCatcher002-SpyTag002 system is an engineered version of SpyCatcher-SpyTag which has some enhanced properties.³⁸

Protein Ligation. The ability to covalently link proteins in order to create protein frameworks, or lower the kinetic barrier between multiple modifications of the same substrate the formation of pseudo protein complexes without introducing none native chemical moieties would be extremely desirable. The SpyCatcher-SpyTag system derivative, SpyLigase-SpyTag-KTag, have been demonstrated to be capable of preparing a chain of affibodies. This was achieved by adding SpyTag to one terminal, and K-tag to the other then inducing isopeptide bond formation. This affibody “polymerization” has been shown to enhance the efficiency in capturing cancer cells.³⁸

Bioconjugation. Another promising application of the Catcher-Tag system is the irreversible conjugation of fluorophores onto targets of interest, or to conjugate fluorophores to other targeting molecules such as antibodies in order to better visualize them. This technology can also be applied in pharmaceutical compounds through the conjugation of drugs to antibodies for targeted drug delivery.³⁹

Protein Stabilization. The studying of proteins has always been a monumental task as their functionality is almost entirely dependent on their ability to stay folded. Proteins can become trapped in inactive local energy minimum folds by relatively small environmental disruptions making studying them in their functional form very difficult. One technique that has been employed is the cyclization of proteins by fusing SpyCatcher to one terminal and SpyTag to the other. Once cyclized, some proteins have shown the ability to find their native fold and regain active after environmental stress as high as 100 °C.⁴⁰

Background Techniques

Protein Expression. Proteins were expressed with two different systems, Auto Induction, and IPTG.

IPTG Expression. The more traditional route of expression is IPTG expression. IPTG expression works through the use of IPTG, isopropyl β -D-1-thiogalactopyranoside. IPTG is imported into the cell much like lactose, and stimulates the expression of proteins on the *lac* operon (**Figure 11**). Unlike lactose, IPTG is not a metabolite and its concentration does not rapidly decrease, allowing for a constant rate of protein expression once IPTG is internalized until cellular death.

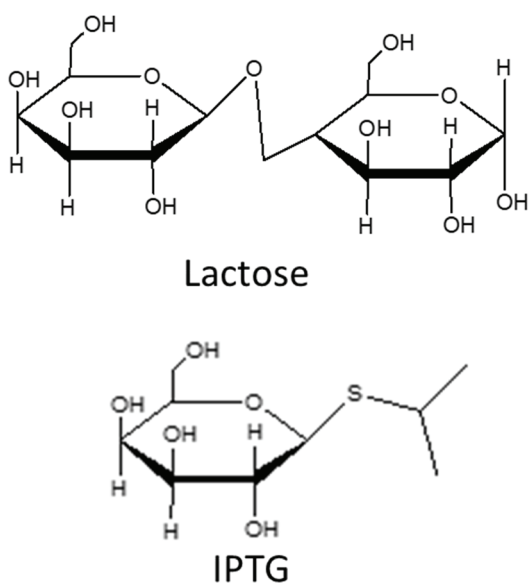


Figure 11. IPTG. Chemical structure of lactose compared to isopropyl β -D-1-thiogalactopyranoside.

Autoinduction. An autoinduction protein expression system was used due to reported decrease in observation time and large cellular density build-up.⁴¹ The autoinduction system used exploited the ability of MgSO_4 to aid in the development of higher cell densities than other expression techniques. Once cell density is built up,

glucose is completely consumed and the import of lactose from the media into the cells stimulates protein expression (**Figure 12**).

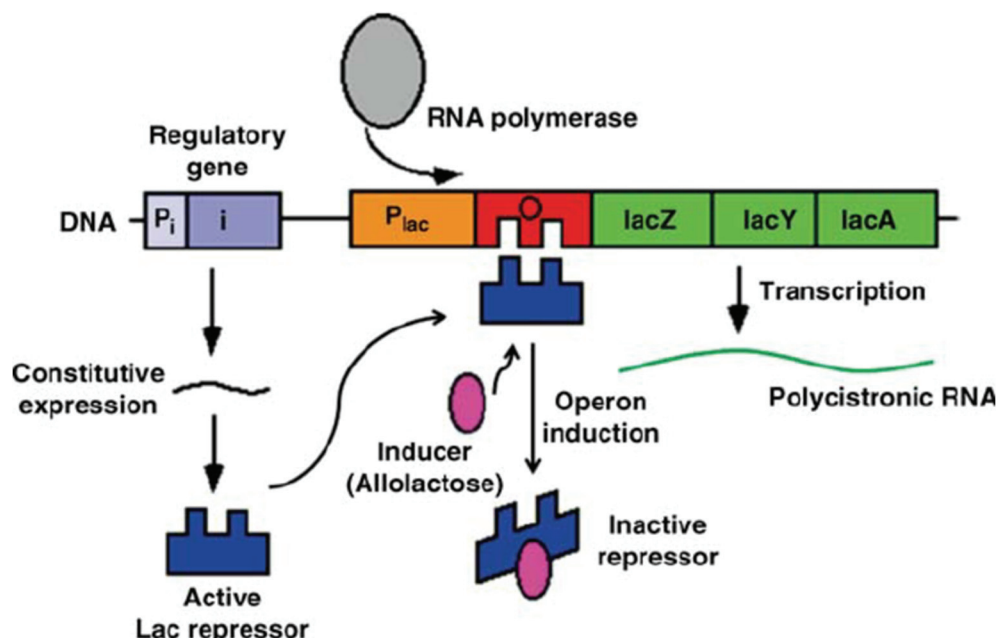


Figure 12. Autoinduction. Metabolite interaction with *lac* operon for promotion of protein expression.⁴¹

Fluorescence Polarization/Depolarization. A key technique used in this work is known as fluorescence polarization/depolarization and relies upon the anisotropy of fluorescence, meaning that if a fluorophore is excited with plane polarized light, it will then emit plane polarized light.⁴² As a fluorophore in solution emits light, the fluorophore itself is in a constant state of motion, or tumbling.⁴² This tumbling causes slight depolarization of the emitted light.⁴² Light polarization can be quantified through a ratio of parallel light, the light in the polarized plain, and perpendicular light, the light that has resulted at all angles due to scattering a depolarization.⁴² Small molecules

tumble much faster so a smaller fluorophore will result in a larger degree of depolarization (**Figure 13**).⁴²

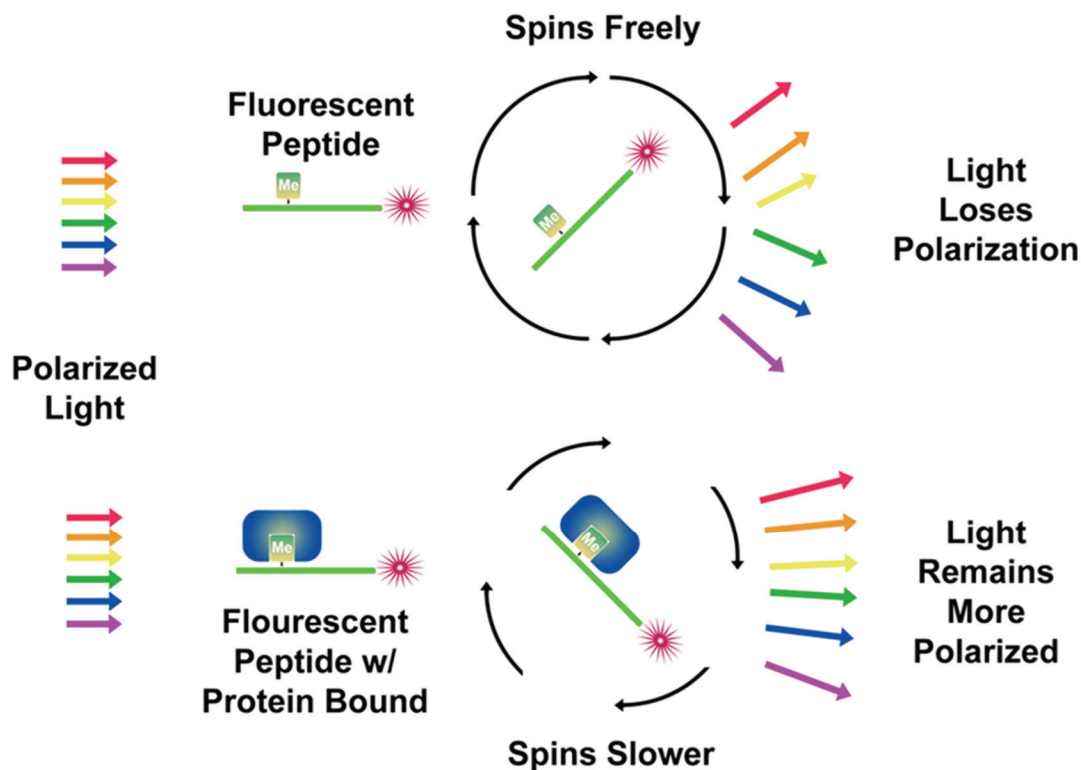


Figure 13. Fluorescence polarization/depolarization. Scheme for the concept behind the technique fluorescence polarization/depolarization.⁴² Rights managed by Taylor & Francis.

In our work we exploited this phenomena in order to observe the change in polarization as a small fluorescent tag binds to a larger partner effectively slowing the tumbling effect. The effects can be quantified in **Figure 14**, where G is an assay and instrument specific value to help standardize absolute values.

$$mP = 1000 * \frac{Parallel - Perpendicular * G}{Parallel + Perpendicular * G}$$

Figure 14. Fluorescence polarization/depolarization quantification. Equation showing the calculation used to find mP or, millipolarization, the unit used for the quantification of fluorescence polarization/depolarization.

Kinetic Study. In order to gain insight into the affinity and bond forming interactions that take place between SpyCatcher-SpyTag model systems needed to be prepared. We expressed SpyCatcher, SpyCatcher EQ, and SpyTag fused proteins, use solid-phase peptide synthesis to synthesize a none-fused SpyTag, and fluorescently label different combinations of these proteins in order to get real time kinetic data through fluorescent polarization-depolarization. In order to perform these tests, two systems were developed.

SpyCatcher-FITC/SpyTagMBP System. The first system used FITC conjugated to lysine side chains on SpyCatcher WT and SpyCatcher EQ. This system though has problems in that the reactive residue on SpyCatcher is a lysine itself. A free SpyTag peptide in this system would not be useful in fluorescence polarization due to the fluorescent body needing to be significantly smaller than its binding partner. To solve this issue, SpyTagMBP was used for its larger size, ~42 kDa.

SpyTag-FITC/SpyCatcher System. The second of these systems was designed on the idea of using solid-phase peptide synthesis to produce SpyTag with an N terminal β -alanine. The β -alanine was added to the SpyTag sequence avoid subsequent eliminations of the FITC molecule by Edman degradation.

Objectives

The objective of our work was to establish a rapid assay to assist the understanding between the affinity interactions and bond formation in the SpyCatcher-SpyTag, and other isopeptide bond forming systems. We hope to develop a rapid assay to accomplish this in hopes of gaining a clear enough idea behind their relationship to aid in the development of specifically engineered protein sites that are capable of irreversibly forming isopeptide bonds with targetable regions of low abundant proteins and peptides. In order to do this, a source of SpyCatcher and SpyTag conjugated proteins were expressed in *E. Coli* using recombinant DNA and studied by using fluorescence polarization/depolarization.

MATERIALS

Chemicals

The following chemicals and instrumentation was used to complete this work.

Agarose (VWR Life Science), 9012-36-6
Bacteriological Agar (Sigma Aldrich), 9012-18-0
Tris-Base (Fischer Scientific), 77-86-1
Sodium dodecyl sulfate (Fischer Scientific), 151-21-3
Ethanol (Ultra Pure), 64-17-5
Glucose (Sigma Aldrich), 50-99-7
Ethylenediaminetetraacetic acid (Fischer Scientific), 6381-92-6
Hydrochloric acid (Fischer Scientific), 7647-01-0
Sodium hydroxide (Fischer Scientific), 1310-73-2
Potassium acetate (Sigma Aldrich), 127-08-2
Acetic acid (Fischer Scientific), 64-19-7
Glycerol (Fischer Scientific), 56-81-5
Sodium chloride (Fischer Scientific), 7647-14-5
LB Media (Fischer Scientific)
Calcium chloride (Fischer Scientific), 10043-52-4
Magnesium chloride (Fischer Scientific), 7786-30-3
Ampicillin (Acros Organics), 69-52-3
Kanamycin (Acros Organics), 25389-94-0
Magnesium sulfate (CHEM-IMPEX INT'L INC.), 7487-88-9
Disodium phosphate (Fischer Scientific Company), 7558-79-4
Monopotassium phosphate (Fischer Scientific), 7778-77-0
Ammonium sulfate (Fischer Scientific), 7783-20-2
 α -lactose (Sigma Aldrich), 5989-81-1
Isopropanol (Fischer Scientific), 67-63-0
SYBR® Safe DNA gel Stain (Invitrogen)
Gel Green Nucleic Acid Stain (BioTium)
Coomassie® Brilliant Blue R-250 (MP Biomedicals), 6104-59-2
Coomassie® Brilliant Blue G-250 (MP Biomedicals), 6104-58-1
Bromophenol Blue (J.T. Baker), 115-39-9
Imidazole (CHEM-IMPEX INT'L INC.), 288-32-4
1 kb DNA Ladder (New England BioLabs® Inc)
Gel Loading Dye Purple 6X, supplied as a component of 1 kb DNA Ladder (New England BioLabs® Inc)
10X Fast Digest Buffer (Thermo Scientific)
1-methyl-2-pyrrolidinone (VWR) 872-50-4
Precision Plus Protein™ Unstained Standards (BIO-RAD) 161-0363
Dimethylformamide (Fischer Chemical), 68-12-2
Fluorescein isothiocyanate, (Thermo Scientific) 3326-32-7

Sodium Bicarbonate (Fischer Chemical), 144-55-8
HisPur™ Ni²⁺-NTA Resin (Thermo Scientific) 88221
Mini-PROTEAN TGX™ Gels 12% (BIO-RAD) 456-1046
Fmoc-Ala-OH (Novabiochem), 35661-39-3
Fmoc-Ile-OH (Novabiochem), 71989-23-6
Fmoc-His(Trt)-OH (Novabiochem), 109425-51-6
Fmoc-Asp(OtBu)-OH (Novabiochem), 71989-14-5
Fmoc-Tyr(tBu)-OH (Novabiochem), 71989-38-3
Fmoc-Val-OH (Novabiochem), 68858-20-8
Fmoc-Met-OH (Novabiochem), 71989-28-1
Fmoc-Lys(Boc)-OH (Novabiochem), 71989-26-9
Fmoc-Thr(Bu)-OH (Novabiochem), 71989-35-0
Fmoc-Pro-OH (Novabiochem), 71989-31-6
Fmoc-β-alanine (CHEM-IMPEX INT'L INC) 02374
NovaPEG Rink Amide resin (Novabiochem)
Bio-Rad Protein Assay Dye Reagent Concentrate (BIO-RAD) 5000006
Bovine Serum Albumin (Sigma)

Kits

E.Z.N.A® Plasmid DNA MiniKit I (Omega bio-tek)

Plasmids (Gifts from Mark Howarth through Addgene, Appendix A)

pDEST14-SpyCatcher
pDEST14-SpyCatcher EQ
pET28a SnoopTag-mEGFP-SpyTag
pET28a SpyTagMBP

Enzymes

*Eco*RI (Thermo Scientific)
*Eco*RV (Thermo Scientific)
*Nde*I (Thermo Scientific)
RNase A (Omega bio-tek)

Bacteria

BL21 (DE3)

Instrumentation

SpectraMax M5

Mikro 22R Hettich Zentrifuge
Applied Biosystems Veriti 96 Well Plate Thermal Cycler
Fischer Scientific Mini Centrifuge
LabDoctor™ 8 MiniFuge by MidSci®
Boekel Scientific Flask Dancer
Incubator
Agilent Technologies Cary 60 UV-Vis
Sorvall Legend X1R Centrifuge Thermal Scientific
Sartorius 0.1 µL- 3 µL pippetor
Sartorius 0.5 µL- 10 µL pippetor
Sartorius 100 µL- 1000 µL pippetor
Sartorius 10 µL – 100 µL pippetor
Autoclave (Primus Sterilizer Co)
Vacufuge
Liberty Blue CEM Microwave Peptide Synthesize

Other Equipment

50 mL Centrifuge Tubes
15 mL Centrifuge Tubes
1.5 mL Micro Centrifuge Tubes
PCR Tubes
Petri Dishes
1 L Media Bottles
500 mL Media Bottles
100 mL Media Bottles
50 mL Media Bottles
1 mL cuvette
250 mL Erlenmeyer flask
100 mL beaker
1 L Erlenmeyer flask
Vacuum Chamber
Vacuum Pump
Rod Sonicator
Hot Water Bath
Thermometer
Nephlo culture flask with side arm
Ethanol Lamp
Flint Striker
-80 °C Freezer
-20 °C Freezer
Clare Chemical Research Dark Reader
Mupid®-2plus Submarine electrophoresis system
3 mL Fritted Syringe (HSW)
96-well plate (greiner bio-one)
3.5 kD MWCO Dialysis Membrane (Spectrum Laboratories, Inc.)

METHODS

General Methods

The general sequence that was needed in this work was done through a linear series of steps consisting of: 1) preparation of the chemically competent cell; 2) plasmid purification; 3) transformation into the chemically competent cell; 4) protein expression; 4) protein purification; 5) confirmation of protein activity; 6) preparation of FITC conjugates; 7) confirmation of FITC conjugate activity; 8) and finally fluorescence polarization/depolarization (**Figure 15**).

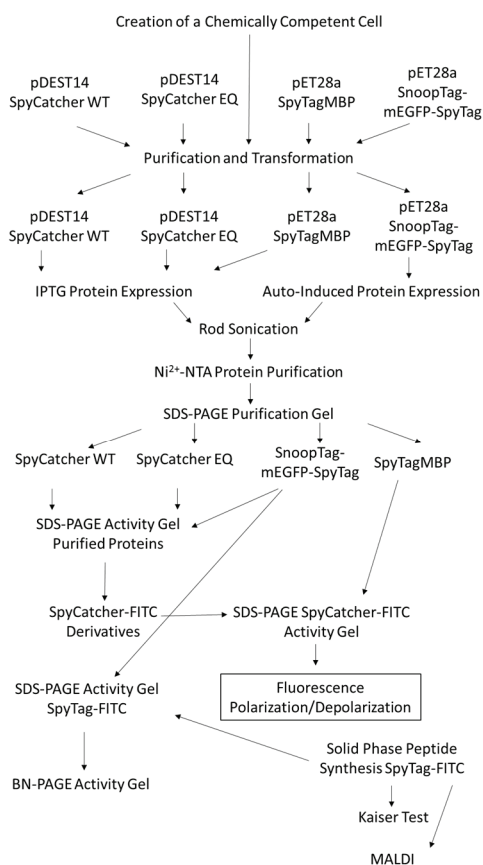


Figure 15. General research scheme. General scheme of procedures performed in this work.

Procedures for General Molecular Biology

Media Dish Preparation. LB plates containing 50 $\mu\text{g}/\mu\text{L}$ of Ampicillin, or Kanamycin were prepared, by dissolving premade LB powder, and bacteriological agar in water at a ratio of 2.5 g: 1 g: 100 mL ddH₂O (~10 plates for 100 mL) scaling with the amount of plates desired. This solution was then autoclaved and briefly allowed to cool before adding a 1000th of the solution volume of desired antibiotic (50 mg/ μL) to the solution, swirling briefly, and then pouring the solution on petri dishes in approximately 10 mL aliquots. The dishes were then allowed to cool and gel. These dishes were then sealed with Parafilm[®] and stored at 4 °C.

Inoculation. Inoculations were performed in 1.5 mL aliquots of LB media transferred aseptically into 13 mm x 100 mm Pyrex[®] glass test tubes. A 1000th of their media volume (1.5 μL) of the appropriate antibiotic at 50 mg/ μL was added to test tubes for selection. The final concentration of antibiotic was 50 $\mu\text{g}/\mu\text{L}$. A sterile toothpick was then used to pick a single colony from its plate. The medium was inoculated by depositing the toothpick into the test tube media. The inoculated media; was then incubated between 15-24 hours at 37 °C on an orbital shaker shaking at 300 rpm (Boekel Scientific Flask Dancer). When performing inoculations, a replica of each colony inoculated was also prepared. For this, before depositing the toothpick in the test tube, the toothpick colony contact point was lightly touched on a premade selection media plate and incubated between 15-24 hours at 37 °C.

Chemically Competent Cell Preparation. Premade LB powder (1.25 g) was placed in a 300 mL Nephlo culture flask with side arm. The LB powder was dissolved in 50 mL of DI water and autoclaved. In parallel, 1.5 mL micro-centrifuge tubes

(approximately 50 tubes) and 50 mL centrifuge tubes (2 tubes) were also sterilized by autoclaving, tubes were then chilled. A 100 mM magnesium chloride solution was prepared by dissolving 2.033 g in 100 mL water. A 100 mM calcium chloride solution was prepared dissolving 1.4701 g in 100 mL water. An 85 mM calcium chloride solution of 15% (v/v) glycerol was prepared by mixing 22 mL of 100 mM calcium chloride solution with 3.3 mL of glycerol. These solutions were chilled and stored at 4 °C.

For pre-culturing 1.5 mL of LB media that did not contain antibiotics was inoculated with a BL21(DE3) colony and incubated at 37 °C on an orbital shaker shaking at 300 rpm (Boekel Scientific Flask Dancer). Once the *E. coli* had grown, after ~20 hours, 1 mL of the grown culture was added to the media prepared in a Nephlo culture flask with side arm culture flask. The flask was then shaken at 200 rpm on the Boekel Scientific Flask Dancer at 37 °C. The optical density at 600 nm (OD_{600}) of the culture was measured every 0.5 to 1 hour. Once the OD_{600} value reaches between 0.350 and 0.400, the flask was placed on ice for 20 minutes. The culture was then split evenly between the two chilled 50 mL centrifuge tubes and centrifuged for 10 minutes at 3,000 x g and 4 °C. Supernatants were discarded through decantation and the pellets were resuspended in 20 mL of chilled 100 mM magnesium chloride solution. The two tubes were combined and centrifuged at 2,000 x g for 10 minutes at 4 °C. The supernatant was discarded through decantation and the pellet was resuspended in 40 mL of 100 mM calcium chloride. This solution was kept on ice for ~40 minutes. The tube was centrifuged at 1,000 x g for 10 minutes at 4 °C. The supernatant was discarded through decantation and the pellet was resuspended in 85 mM calcium chloride containing 15% (v/v) glycerol. This solution was then dispensed in aliquots of 50 μ L to the 1.5 mL

micro-centrifuge tubes. The micro-centrifuge tubes containing the prepared competent cell aliquots were stored in the -80 °C freezer.

Procedures for DNA Handling

Mini-Prep (Plasmid DNA Extraction). The 1.5 mL *E. coli* culture(s) was transferred from the test tube(s) into a 1.5 mL sterile micro-centrifuge tube(s). This tube(s) was then centrifuged at 15,000 rpm on the Mikro 22R Hettich Zentrifuge at 4 °C for 30 seconds. Once removed, the supernatant(s) was discarded and the micro-centrifuge tube was tapped on a paper towel to remove the last remnants of supernatant. The pellet(s) and solutions from this point forward were kept on ice or at 4 °C for the remainder of this experiment unless stated otherwise. The pellet(s) was suspended in 100 µL of Mini-Prep Solution I (50 mM glucose, 25 mM Tris-HCL pH 8.0, and 10 mM EDTA pH 8.0). A 200 µL aliquot of Mini-Prep Solution II (0.2 M NaOH and 1% SDS) was then added. The micro-centrifuge tube(s) was inverted several times slowly to insure mixing. The tube(s) was placed on ice for 5 minutes. Next, 150 µL of Mini-Prep Solution III (3 M Acetate buffer pH 4.8) was added with slow inversions. The tube(s) was again placed on ice for 5 minutes. The sample(s) was then centrifuged at 15,000 rpm for 3 minutes. The supernatant(s) was transferred to a new, sterile micro-centrifuge tube. Seven-hundred microliters (700 µL) of cold pure ethanol supernatant(s) was added to the supernatant and centrifuged at 15,000 rpm for 10 minutes. The supernatant(s) was removed and the pellet(s) was washed twice with cold 70% ethanol and centrifuged at 15,000 rpm for 1 minute. The pellet(s) was then dried in a vacuum for 10-15 minutes and suspended in 20 µL of sterile DI water.

Kit Mini-Prep. E.Z.N.A® Plasmid DNA MiniKit I was used in situations where higher degrees of purification were needed such as when samples were sequenced and follows the same principles as non-kit Mini-Prep so only the differences will be highlighted below: 1) the pellet(s) was suspended in 250 μ L of Mini-Prep Solution I containing RNase; 2) two-hundred and fifty microliters (250 μ L) of Mini-Prep Solution II was used; 3) three-hundred and fifty microliters (350 μ L) of Mini-Prep Solution III was used; 4) supernatant was moved into a Hibind® Column(s) previously prepped with 100 μ L of 3 M NaOH instead of a new, sterile micro-centrifuge tube. The column(s) was placed in a new, sterile micro-centrifuge tube(s) and centrifuged at 15,000 x g for 1 minute with filtrate being discarded afterward. A 500 μ L portion of HBC buffer with isopropanol was added to the column(s) and centrifuged through at 15,000 x g for 1 minute with the filtrate being discarded. The column(s) was then washed through twice with 700 μ L of DNA wash buffer containing ethanol. Each wash included spinning at 15,000 x g for 30 seconds and discarding the filtrate. Finally, the column(s) was centrifuged at 15,000 x g for 2 minutes to dry. For elution, 20 μ L of sterile DI water was added to the column(s) and centrifuged at 15,000 x g for 1 minute (**Figure 16**).

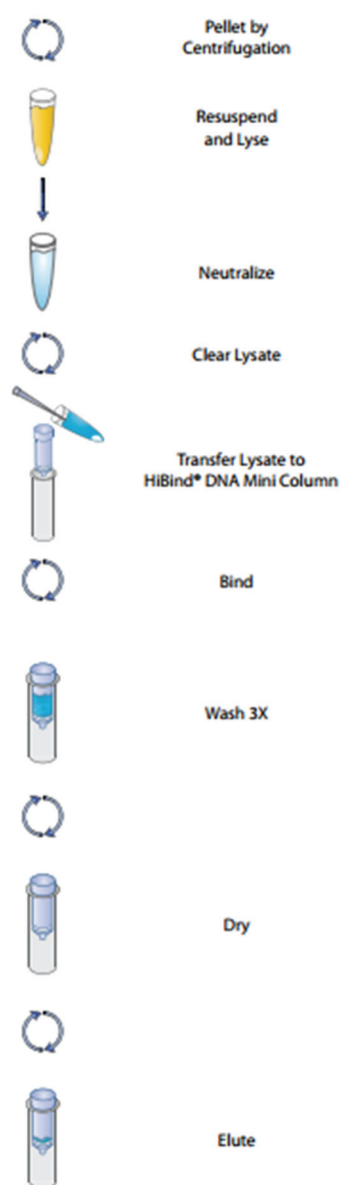


Figure 16. E.Z.N.A. Kit Mini-Prep. Scheme for steps of kit plasmid purification.⁴³

Plasmid Digestion. Purified plasmids were digested by mixing 7 μ L sterile DI water, 1 μ L of 10X Fast Digest Buffer, 1 μ L plasmid sample, and 1 μ L Restriction Enzyme in a PCR tube. The solution was then incubated in the Applied Biosystems Veriti 96 Well Plate Thermal Cycler at 37 °C for 1 hour. The sample was then kept on ice until it was prepared for electrophoretic analysis.

Agarose Gel Electrophoresis. The following procedure was used for the electrophoresis. If more samples were needed, agarose and buffer amounts were doubled and a 16 well gel was made.

Agarose Gel Preparation (for an 8 well gel). Agarose was weighed out into a 125 mL Erlenmeyer flask to a mass of 0.25 g. This was then dissolved in 25 mL of TAE buffer (40 mM Tris, 20 mM acetic acid, and 1 mM EDTA, pH 8.3) by heating in a microwave oven for 30 seconds. The solution was allowed to cool until it could be held bare handed. The solution was then poured into a casting tray and a comb was inserted. The gel was allowed to solidify over the next 30-50 minutes. Once the gel solidified, the comb was slowly removed and the gel, along with the casting tray, was placed into a Mupid[®]-2 plus Submarine electrophoresis system. The gel was faced so the wells were on the side of the cathode. TAE buffer was used to fill the electrophoresis chamber until the liquid level was slightly above the gel surface.

Sample Running. Digested plasmid samples (10 μ L) were then loaded into the wells after mixing with Gel Loading Dye Purple 6X (2 μ L) in proportions to bring the dye to 1X. For the 1 kb DNA Ladder, 1 μ L of the ladder solution was mixed with Gel Loading Dye Purple 6X (1 μ L) and 4 μ L of sterile DI water before being loaded to a well. Once all samples had been loaded, the chamber was closed and run at the voltage setting of “half”. Once the loading dye had reached the opposite end of the gel, the chamber was turned off and the gel was submerged in a solution of either Gel Green Nucleic Acid Stain, or SYBR[®] Safe DNA gel Stain, and incubated for ~30 minutes. The image of the gel was captured on a dark reader with a camera.

Transformation. One microliter (1 μL) of plasmid solution at around 30 ng/ μL was added to a tube containing 50 μL of chemically competent cells on ice. This was incubated on ice for 5 minutes. The cells were then heat shocked by submersion in a hot water bath at 43 $^{\circ}\text{C}$ for exactly 30 seconds and then placed on ice for 2 minutes. Eighty microliters (80 μL) of LB media was then added to the tubes and incubated at 37 $^{\circ}\text{C}$ for 1 hour with shaking at 150 rpm. Several times during incubation, the cells were flicked to insure mixing. After incubation, the cells were then mixed by pipetting up and down several times. The cells were then spread evenly across an antibiotic containing LB plate and incubated overnight at 37 $^{\circ}\text{C}$.

Procedures for Protein Handling

Protein Expression with Autoinduction.⁴⁷ Premade LB powder (2.5 g) was dissolved in 100 mL water in a 500 mL Erlenmeyer flask. This flask was then autoclaved. Desired selection antibiotics (100 μL) was added to the 500 mL Erlenmeyer flask along with 2 mL of 5052 (0.5% glycerol (w/v), 0.05% Glucose (w/v), 0.2% α -lactose(w/v)), 5 mL of NPS (50 mM Na_2HPO_4 , 50 mM KH_2PO_4 , 25 mM $(\text{NH}_4)_2\text{SO}_4$), and 0.1 mL of 2 M MgSO_4 . The final concentration of the antibiotics was 50 $\mu\text{g/mL}$. For pre-culturing 1.5 mL of LB media containing appropriate antibiotics (50 $\mu\text{g/mL}$) was inoculated with *E.coli* strain and incubated at 37 $^{\circ}\text{C}$ on an orbital shaker shaking at 300 rpm (Boekel Scientific Flask Dancer). Once the *E. coli* had grown, after ~20 hours, 1 mL of the grown culture was added to the media prepared in the Erlenmeyer flask. The flask was then shaken at 300 rpm on the orbital shaker at 27 $^{\circ}\text{C}$. Samples were taken periodically to monitor the growth by measuring the OD_{600} . Once the optical density had

reached it plateau, the Erlenmeyer flask was incubated further for an additional 6-10 hours. The contents of the Erlenmeyer flask were then transferred evenly to pre-weighed 50 mL centrifuge tubes and centrifuged at $4,696 \times g$, $4^{\circ} C$ for 10 minutes. The supernatant was then discarded by decantation. The pellets were washed with 0.9% NaCl twice by resuspension and centrifugation at $4,696 \times g$, $4^{\circ} C$ for 10 minutes. The pellets were stored in the $-80^{\circ} C$ freezer.

Protein Expression IPTG. Premade LB powder (2.5 g) was dissolved in 100 mL water in a 500 mL Erlenmeyer flask. This flask was then autoclaved. Desired selection antibiotics (100 μL) was added to the 500 mL Erlenmeyer flask. The final concentration of the antibiotics was 50 $\mu g/mL$. For pre-culturing 1.5 mL of LB media containing appropriate antibiotics (50 $\mu g/mL$) was inoculated with *E.coli* strain and incubated at $37^{\circ} C$ on an orbital shaker shaking at 300 rpm (Boeckel Scientific Flask Dancer). Once the *E. coli* had grown, after ~ 20 hours, 1 mL of the grown culture was added to the media prepared in the Erlenmeyer flask. The flask was then shaken at 300 rpm on the orbital shaker at $38^{\circ} C$. Careful track of bacterial growth was kept through the periodic checking of OD_{600} . Once the OD_{600} had reached between 1.5 and 2.0, 500 μL of 100 mM IPTG was added and the culture was incubated on an orbital shaker at 300 rpm at room temperature overnight. The culture was then transferred to two 50 mL centrifuge tubes and the tubes were centrifuged at $4696 \times g$ at $4^{\circ} C$ for 10 minutes. Supernatant was discarded by decantation. Pellets were washed in 0.9% NaCl through resuspension and centrifugation at $4696 \times g$ ($4^{\circ} C$). This was repeated 3 times. Pellets were then stored in the $-80^{\circ} C$ freezer unless used immediately (**Table 1**).

Table 1. IPTG OD_{600} . The OD_{600} met by each strain of bacteria cultured in IPTG protein expression before the addition of IPTG

Strain	OD_{600}
BL21(DE3)/pDEST14-SpyCatcher WT	1.862
BL21(DE3)/SpyCatcher EQ	1.912
BL21(DE3)/pET28a-SpyTag MBP	1.630

Protein Extraction. Cell pellets were suspended in a volume of phosphate buffer pH 6.99 equal to twice the gram mass of the pellet in mL (2 mL for every 1 g of cell). The cell suspension was then kept on ice while it was sonicated with a rod sonicator to prevent excessive heating of the protein sample. This was typically done in 5 sets of 2 minute sonication where sonication would continue for 2 minutes straight before being allowed to cool back down (approximately 10 minutes). The sample was then centrifuged at 15,000 x g, and the pellet was inspected. If the pellet had a lighter, loosely packed, top after centrifugation, it was resuspended and sonicated again. This was continued until the pellet was completely dark and well packed after centrifugation. Supernatant was collected and mixed 1:1 with a 50% glycerol solution. The crude cell extracts was then stored in the -80 °C freezer.

Protein Purification. One milliliter (1 mL) spin columns were packed by adding 400 μ L of Ni^{2+} -NTA slurry to the column and centrifuging at $700 \times g$ for 2 minutes in 1.5 mL centrifuge tubes. This would generally produce a resin bed of approximately 200 μ L. For larger scale, a 10 mL spin column in a 15 mL centrifuge tube packing with 2 mL of Ni^{2+} -NTA slurry produced a 1 mL resin bed. Twice the resin volume of equilibration buffer (25 mM sodium phosphate buffer, 500 mM NaCl, 10 mM imidazole, pH 7.0) was

run through the column by centrifugation at $700 \times g$, this was repeated one more time. One resin volume of crude cell extract was then added to the column and the column was centrifuged at $700 \times g$ for 2 minutes. The flow through from this step was reloaded into the column and centrifuged again at $700 \times g$ for 2 minutes. The flow through after second loading was collected and stored in the $-20\text{ }^{\circ}\text{C}$ freezer for later use. Weakly associated proteins were washed off with one resin volume of wash buffer (25 mM sodium phosphate buffer, 500 mM NaCl, 20 mM imidazole, pH 7.0) centrifuged at $700 \times g$ for 2 minutes. The wash step was repeated three times, and all fractions were collected. Two resin volumes of elution buffer (25 mM sodium phosphate buffer, 300 mM NaCl, 250 mM imidazole, pH 7.0) was then passed through the column by centrifugation at $700 \times g$ for 30 seconds, this was done 5 times and fractions for each were collected. Elution fractions were dialyzed against ten times volume of 10 mM PBS changed every 8 hours for three changes. All fractions for each step were stored in the $-20\text{ }^{\circ}\text{C}$ freezer (**Figure 17**).

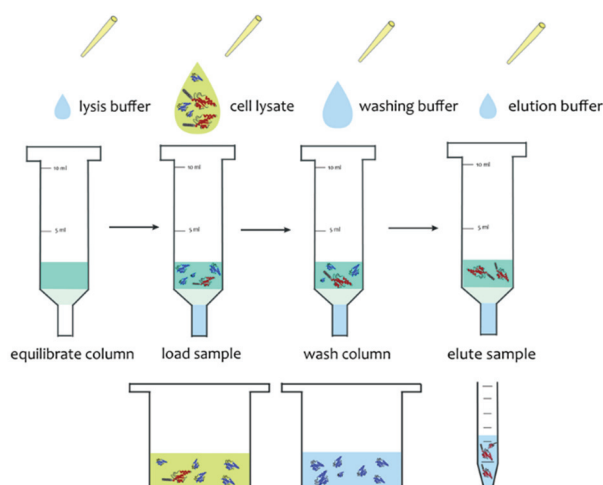


Figure 17. Ni^{2+} -NTA. Scheme of Ni^{2+} -NTA purification.⁴⁵

SDS-PAGE. Four (4)X SDS sample loading buffer was prepared by mixing 1.6 mL of bromophenol blue, 3.3 ml of glycerol, 25 mL of 1 M Tris-HCl (pH 6.8), 0.5 mL of DI water, 1 g of SDS, and 2 mL of 2-mercaptoethanol. Sample volumes were determined based on the result of Bradford Assay. Typically for purified protein samples, 0.5-5 μ L of 1 mg/mL protein samples were mixed with \sim 3 μ L of 4X SDS loading buffer. The total volume of the mixture was adjusted to 12 μ L by addition of the water and incubated at 95 $^{\circ}$ C for 10 minutes. For crude samples, a smaller volume was used due to higher protein concentrations (*e.g.* 0.5-1 μ L of 3-6 mg/mL in total protein concentration).

A precast gel was then placed in the vertical gel electrophoresis apparatus and filled with SDS running buffer until the bottom of the gel was in contact. The samples were then loaded into the wells and the apparatus was run at a constant 73 V. Once the dye from the SDS loading buffer reached to the bottom of the gel, the gel was removed carefully. For fluorescent samples, pictures were taken on a darkreader with a camera.

The gel was then submerged in prestaining solution (20% methanol, 7.5% glacial acetic acid, 72.5% DI water) (v/v/v) for 15 minutes. The gel was then transferred to staining solution (125 mL methanol, 12.5 mL glacial acetic acid, 112.5 mL DI water, and 0.625 g Coomassie Brilliant Blue R-250) for 30 minutes. Finally, the gel was transferred to destaining solution (12.5 mL methanol, 17.5 mL glacial acetic acid, and 220 mL DI water) and incubated overnight. The image of the stained gel was captured on a white light transilluminator with a camera.

Blue Native PAGE (BN-PAGE).⁴⁶ Blue native PAGE was performed using a running buffer consisting of 1.5 g tris-base and 7.2 g glycine in 500 mL DI water. Loading buffer was prepared with 15 mL running buffer, 0.15 g Coomassie Blue G-250,

and 5 mL glycerol. Before gel loading, samples were mixed with up to 10 μ L DI water, and 2 μ L loading buffer was added. Mini-PROTEAN® TGX™ precast gels were used and run at 73 V until dye front was near the end of the gel. For fluorescent samples, pictures were taken on a darkreader with a camera. The gel was then placed in prestaining solution (20% methanol, 7.5% glacial acetic acid, 72.5% DI water) (v/v/v) for 15 minutes. The gel was then moved to Staining solution (125 mL methanol, 12.5 mL glacial acetic acid, 112.5 mL DI water, and 0.625 g Coomassie Brilliant Blue R-250) for 30 minutes. Finally, the gel was moved to destaining solution (12.5 mL methanol, 17.5 mL glacial acetic acid, and 220 mL DI water) and incubated overnight. The image of the stained gel was captured on a white light transilluminator with a camera.

Bradford Assay. Bradford Assays were performed using a 96-well microplate on a microplate reader. BSA standards were prepared by adding 0, 0.50, 0.75, 1.0, 1.5, 2.0, 2.5, and 3.5 μ L of 1.0 mg/mL BSA solution to each well. Sterile DI water was also added to the wells in order to adjust the total volume to be 10 μ L. The final concentration of the standard ranged from 0 to 350 μ g/mL. Serial dilutions of samples were prepared, and 10 μ L of each diluted sample was added to separate wells. Two-hundred microliters (200 μ L) of 1:4 diluted Bio-Rad Protein Assay Dye Reagent Concentrate was added to each well and after 5 minutes, absorbance at 595 nm was taken. Both standards and samples were measured in triplicate.

Fluorescence Polarization/Depolarization System Development

FITC-Labeling of SpyCatcher WT and SpyCatcher EQ. Prior to the reaction, protein samples were dialyzed against phosphate buffer saline (PBS) (pH 7.4). A

solution of 10 mg/mL FITC (fluorescein isothiocyanate) was prepared in DMSO. Immediately before the reaction, 20 μ L of the 1 M sodium bicarbonate solution was added for every 200 μ L of protein solution. For every 0.25 mg of protein, 1 μ L of FITC solution was added. This reaction was left to proceed overnight. The reaction vessel was covered to protect the sample from light. On the following day, solutions were dialyzed against PBS of 1000 times volume. The dialysis solution was changed every 8 hours for 3 times. The protein samples were concentrated by using a vacuufuge at room temperature until a desired concentration (\sim 1 mg/mL) was achieved. The sample was dialyzed against PBS, and solutions were stored at 4° C.

Solid-phase Peptide Synthesis. SpyTag was synthesized on a solid-phase peptide synthesizer with the addition of β -alanine to the N-terminal ($\text{H}_2\text{N}-\beta\text{-Alanine-A-H-I-V-M-V-D-A-Y-K-P-T-K-CONH}_2$). In order to accomplish this, 0.196 g of a Rink amide resin was used in conjunction with the step wise addition of protected amino acids dissolved in NMP (*N*-Methyl-2-pyrrolidone). The concentration of protected amino acids were at 0.2 M, and 1.25 mL of the solution was used in each coupling cycle (**Figure 18**). Deprotection solution was prepared by dissolving 20 g of piperazine and 5.65 g of oxyma pure in NMP. Deprotection steps were carried out with 5 mL of the deprotection solution. Activator solution was composed of 6.24 mL of DIC and 73.76 mL of NMP. The activator base solution was made by dissolving 8.52 g of oxyma pure in 60 mL NMP. One (1) mL and 0.5 mL of activator and activator base solution, respectively were used in each coupling cycle. Wash steps used 5 mL of NMP. N-terminal Fmoc-protection group was deprotected in the last cycle. After completion of peptide synthesis, the resins were transferred into two fritted syringes and then rinsed with \sim 20 mL of

DCM. The resins inside the syringes were dried under vacuum for ~20 minutes. The samples were then stored in an air tight container in the -20° C freezer.

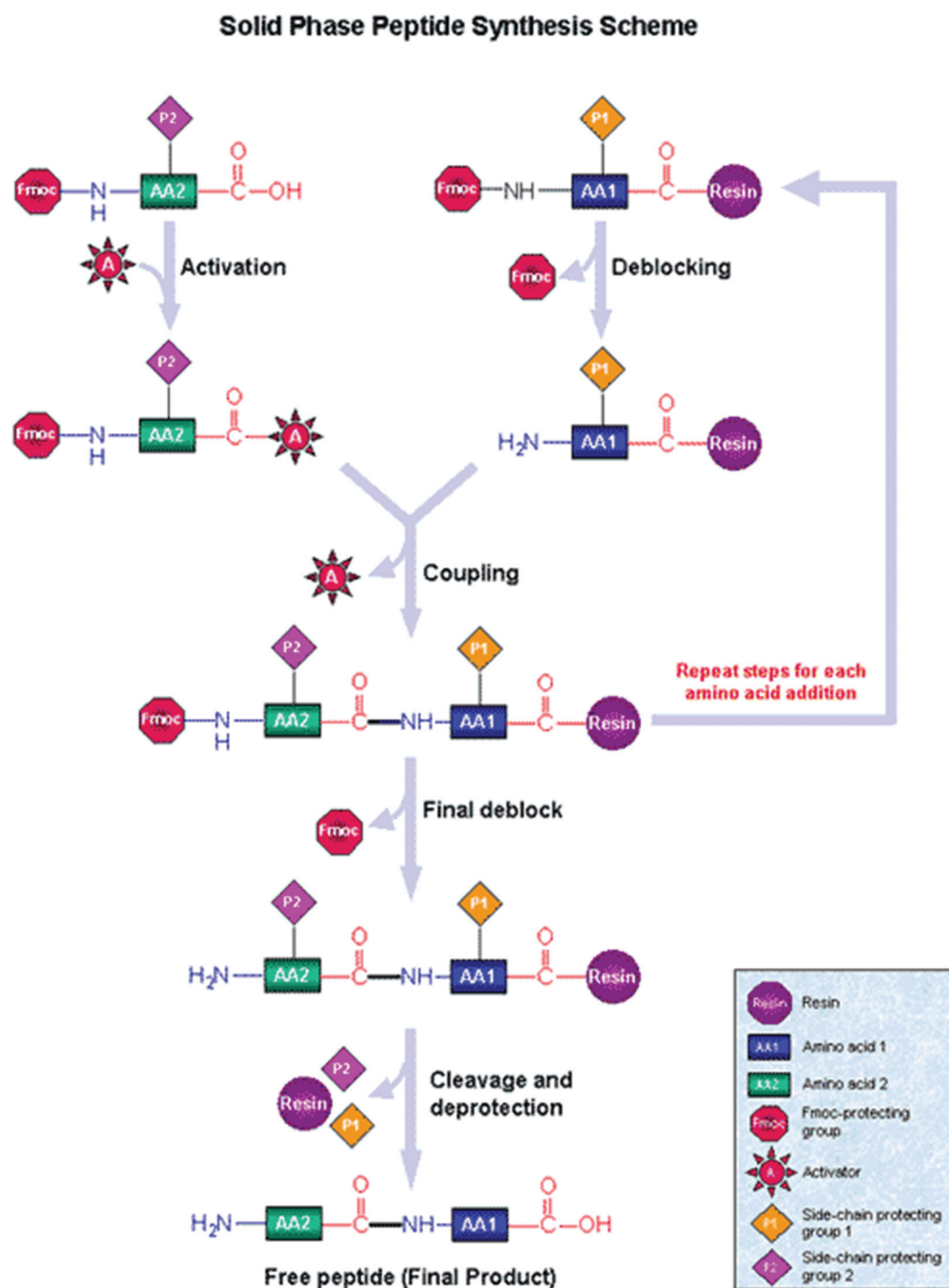


Figure 18. Solid-phase peptide synthesis. Scheme of solid-phase peptide synthesis using Fmoc protecting groups.⁴⁷

Peptide Fluorophore Conjugation. The resins with the synthetic peptides were swelled inside one of the syringes with DCM for ~10 minutes. DCM was then drained and a solution containing 558 μL of NMP, 399 μL of DCM, 43 μL of DIPEA (*N,N*-Diisopropylethylamine), and 0.0487 g of FITC (Fluorescein isothiocyanate) was withdrawn into the syringe and incubated on an orbital shaker overnight at room temperature. The reaction mixture was then drained through the frit and the resins were rinsed with ~20 mL of DCM. The resins inside the syringe were dried under vacuum for ~20 minutes. The sample was then stored in an air tight container in the -20°C freezer (Figure 19).

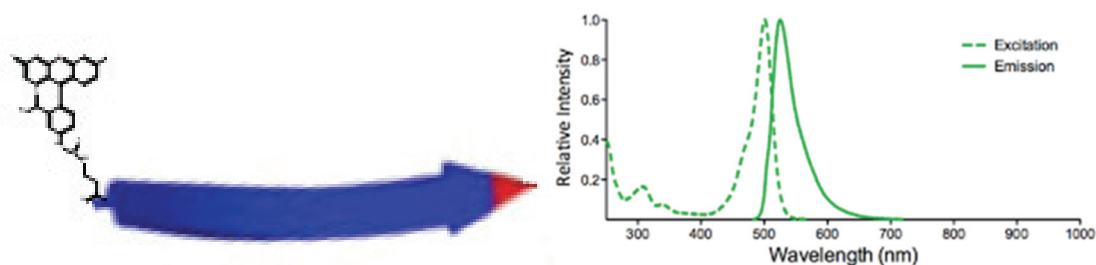


Figure 19. SpyTag-FITC. Visualization of FITC fused SpyTag (left) and FITC excitation emission spectra (right)

Kaiser Test. Several resin beads were transferred into small test tubes. Solution I was prepared by dissolving 0.5 g ninhydrin in 10 mL ethanol. Solution II was prepared by mixing 2 μL of 0.1 M potassium cyanide, 198 μL of DI water, and 10 mL of pyridine. One-hundred microliters (100 μL) each of solutions I and II were added to the test tubes and then heated to 115°C in a silicone oil bath for 5 minutes (Figure 20).

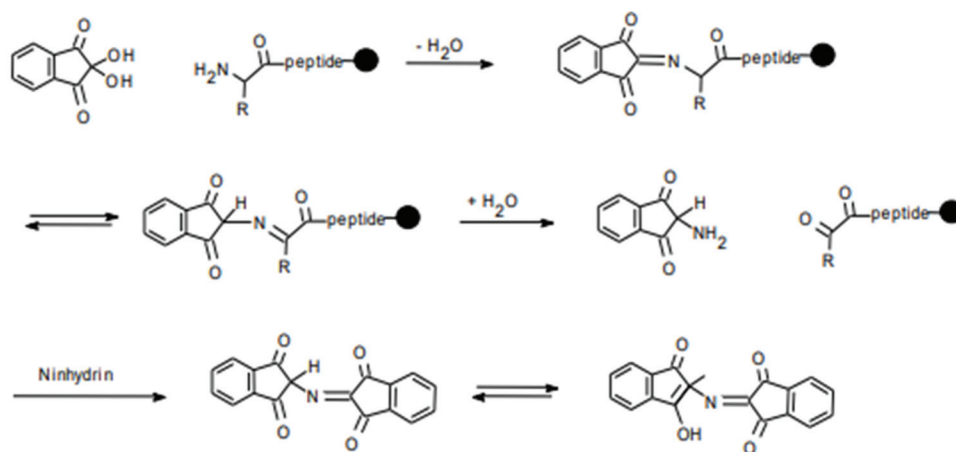


Figure 20. Ninhydrin reaction. Proposed reaction mechanism of ninhydrin with primary amines that makes dark blue color.⁴⁸

Peptide Cleavage. A cleavage cocktail of 9.25 mL trifluoroacetic acid, 0.25 mL of triisopropylsilane, 0.25 mL 3,6-dioxa-1,8-octanedithiol, and 0.25 mL DI water was prepared. Three milliliters (3 mL) of cleavage cocktail was withdrawn into the fritted syringe containing the resin beads. The syringe was capped and incubated on an orbital shaker, set at ~70 rpm, for 3 hours. The supernatant was collected into three 15 mL centrifuge tubes. Each tube received approximately 1 mL of the supernatant. Nine milliliters (9 mL) of cold diethyl ether was added into each tube. The precipitates were collected as pellets by centrifugation at 3,500 rpm for 3.5 minutes. The pellets were rinsed by resuspension in 9 mL of cold diethyl ether followed by centrifugation at 3,500 rpm for 3.5 minutes. The pellets were rinsed 3 times in total. Pellets were then flicked in the tubes to break them up. Kimwipes were used to enclose the tube mouths with rubber bands and then the samples were dried under vacuum over 45 min. The dried peptide was stored in air tight containers in the -20 °C freezer.

Fluorescence Polarization/Depolarization

The degree of fluorescence polarization/depolarization (FP) was determined by using the following equation: $mP = 1000 * (Parallel - Perpendicular * G) / (Parallel + Perpendicular * G)$ where “Parallel” and “Perpendicular” are the fluorescence intensity of the parallel and perpendicular, respectively, polarized light relative to the excitation light, and G is assumed to be one.

SpyTag Concentration Dependence. FP was measured on a Spectramax M5 at room temperature. The concentration dependence of FP was determined by altering the amounts of SpyTagMBP while keeping the amount of SpyCatcher WT-FITC constant at (2 μ L of 0.66 mg/mL). SpyTagMBP, SpyCatcher WT-FITC, and PBS were mixed to prepare two-hundred microliters (200 μ L) of sample solution inside the wells of a 96 well plate in quadruplicate and incubated for 2 hours before FP measurements. The samples were excited at 480 nm and the emission at 535 nm was measured with a 515 nm cutoff filter. The final concentration of SpyCatcher WT-FITC was 413 μ M.

Kinetic Study of Fluorescence Polarization/Depolarization. A kinetic study was performed at room temperature by mixing 0.51 : 1 in mole equivalence of SpyTagMBP and SpyCatcher WT-FITC in quadruplicate. In this study, a SpectraMAX M5 microplate reader was used to measure FP. The plate was shook on the plate reader for 5 seconds before the first measurement. Data points were collected every 30 seconds over 1 hour. SpyTagMBP stock solution (1.5 μ L of 1.2 mg/mL in PBS) and SpyCatcher stock solution (2 μ L of 0.66 mg/mL in PBS) were added simultaneously to 196.5 μ L of PBS (pH 7.4). The final concentration of SpyTagMBP and SpyCatcher WT-FITC was 220 μ M, and 413 μ M, respectively.

RESULTS AND DISCUSSION

Protein Preparation

Four proteins (SpyCatcher-Wild Type, SpyCatcher-EQ, SnoopTag-mEGFP-SpyTag, SpyTag-MBP) were expressed and purified in this work. Preparation of proteins involves purification of plasmids, transformation of chemically competent *E. coli* cells by the plasmids, expression of proteins in the host cells, and purification of the expressed proteins by using immobilized metal ion affinity chromatography (**Figure 21**).

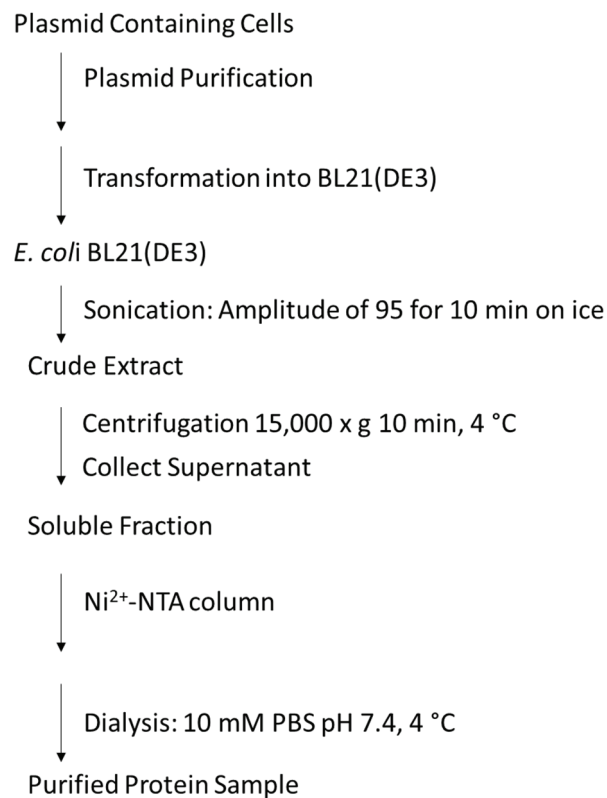


Figure 21: Protein preparation. General scheme for the preparation of proteins.

Preparation of SpyCatcher-Wild Type. The first protein purified in this work was SpyCatcher Wild Type, or SpyCatcher WT.

Preparation of BL21(DE3)/pDEST14-SpyCatcher Strain. **Figure 22** shows the result of agarose gel electrophoresis for pDEST14-SpyCatcher. The plasmid was extracted from BL21(DE3)/pDEST14-SpyCatcher and digested with *EcoRI* before the electrophoresis. The bands in lanes 2 and 3 agreed with the previously reported size of pDEST14-SpyCatcher plasmid (4061 bp). On the other hand, we attributed the smears near the bottom of the gel as RNA contaminants as our kit-free Mini-Prep protocol does not employ RNase.

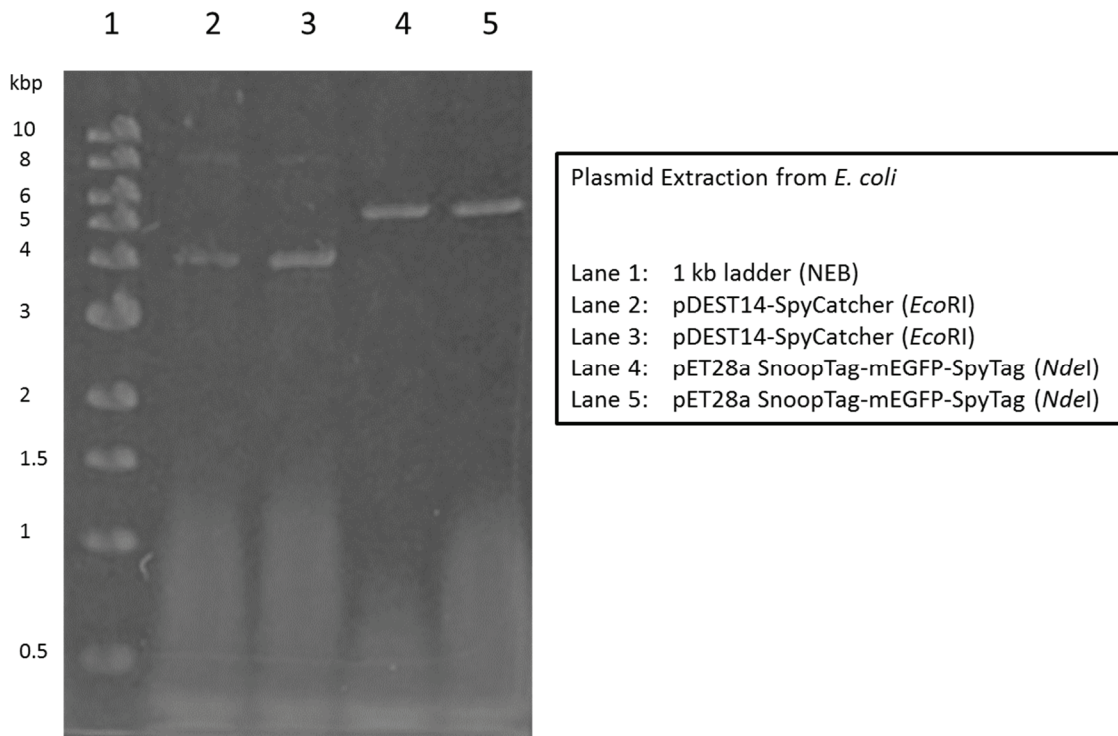


Figure 22. Electrophoresis of pDEST14-SpyCatcher and pET28a SnoopTag-mEGFP-SpyTag on 1% agarose gel. Lane 1: 1 kb DNA Ladder (New England BioLabs®). Lanes 2 and 3: pDEST14-SpyCatcher (4061 bp) digested with *EcoRI*. Lanes 4 and 5: SnoopTag-mEGFP-SpyTag (6154 bp) digested with *NdeI*.

Expression of SpyCatcher WT. **Figures 23** and **24** show the OD_{600} of the culture media during the expression of SpyCatcher-Wild Type in BL21(DE3)/pDEST14-SpyCatcher cells by autoinduction and by the addition of IPTG, respectively.

When BL21(DE3)/pDEST14-SpyCatcher was inoculated in the autoinduction medium, the *E. coli* cells grew up to only a moderate cell density (OD_{600} around 6.0) even after 50 hours. The weight of the harvested cells was 1.4388 g (in wet weight). This result was reproduced in another attempt while the identical medium yielded a high OD_{600} (>14) within 24 hours for the BL21(DE3)/pDEST14-SpyCatcher T51A mutant (**Figure 23**).

SpyCatcher-Wild Type was also expressed by an IPTG expression system. OD_{600} of BL21(DE3)/pDEST14-SpyCatcher reached around OD_{600} 2.0 after 3 hours. At this point, IPTG was added to induce the expression of proteins (**Figure 24**). A wet weight of 1.2007 g was harvested from this culture.

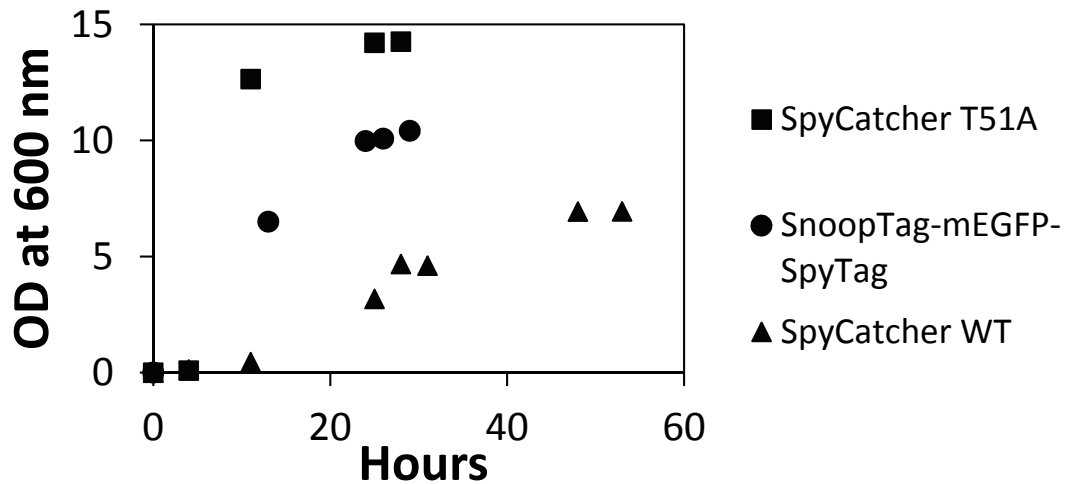


Figure 23. Autoinduction cell growth curve. OD_{600} of BL21(DE3)/pDEST14-SpyCatcher (Wild Type), BL21(DE3)/pDEST14-SpyCatcher T51A mutant, and BL21(DE3)/pET28a SnoopTag-mEGFP-SpyTag during autoinduction expression at 27 °C, 300 rpm

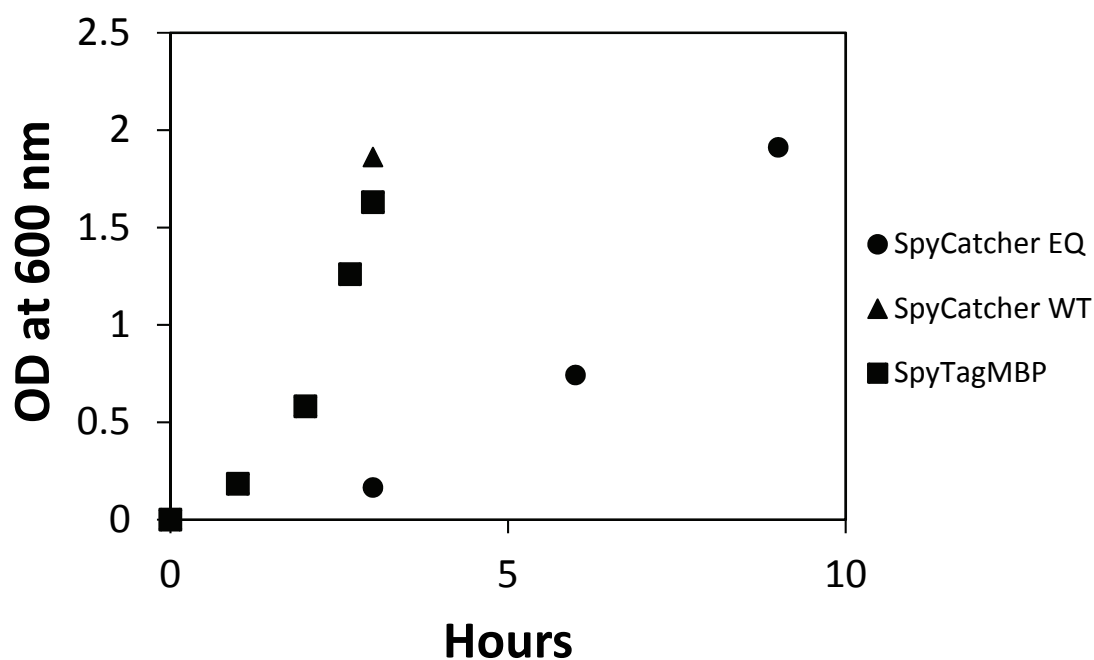


Figure 24. IPTG cell growth curve. OD_{600} of BL21(DE3)/pDEST14-SpyCatcher (Wild Type), BL21(DE3)/pDEST14-SpyCatcher EQ mutant, and BL21(DE3)/pET28a SpyTagMBP before addition of IPTG at 38 °C, 300 rpm.

Purification of SpyCatcher WT. After dialysis, 8 tubes containing approximately 400 μ L of 1.7 mg/mL-0.46 mg/mL SpyCatcher WT samples were obtained. SpyCatcher WT (**Figure 25**), the active non-mutated binding partner to SpyTag, showed several fairly intense bands in lane 2, though the more intense band was at ~16 kDa which is what is expected for SpyCatcher WT. Most protein impurities were removed in the flow through fractions, but a band can be seen at ~37 kDa in the wash lane that shows none specific binding to the column. This protein was removed in the wash fractions and the final elution fraction contained only one clear band in the place of the protein of interest, ~16 kDa. Upon closer observation there seems to be a faint band located just above the intense SpyCatcher band, this has been reported by others, and it has been contributed to by post translational modification of some SpyCatcher proteins.

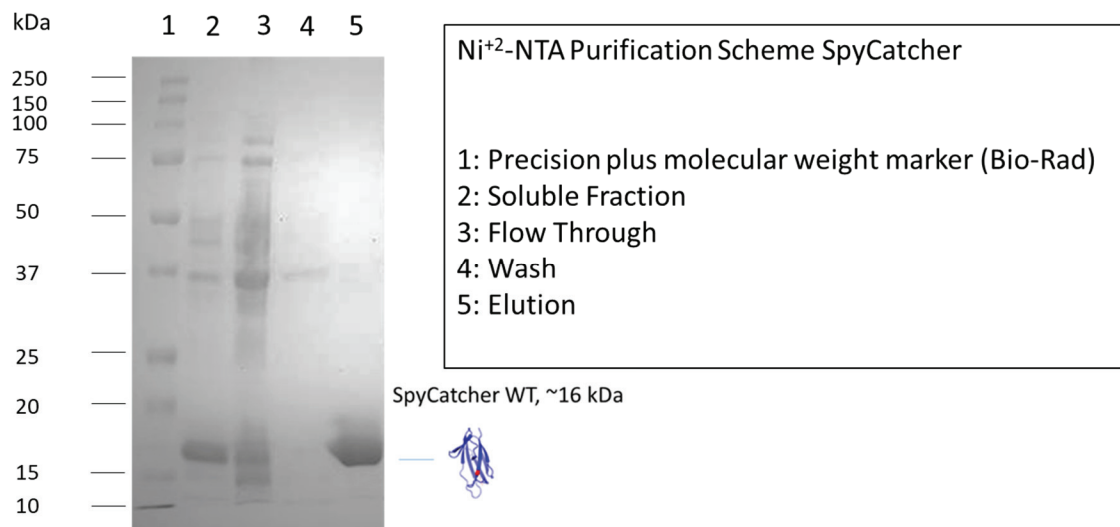


Figure 25. SDS-PAGE of each fraction during the purification of SpyCatcher WT. Purification steps of SpyCatcher WT. Lane 1: Precision plus molecular weight marker (Bio-Rad). Lane 2: soluble fraction. Lane 3: flow through of soluble fraction. Lane 4: wash fraction. Lane 5: elution fraction.

Determination of SpyCatcher WT Expression Success. From the ~0.5 g wet weight of the cell pellet produced from autoinduction, 0.0257 mg of SpyCatcher WT was obtained. This was determined by using Bradford Assay with a BSA standard. On the other hand, IPTG expressed SpyCatcher WT was purified from a pellet of about 0.5 g wet weight, resulting in ~ 3.54 mg of purified protein. This purified protein translates into about 24.5% of the total protein found in the soluble fraction during protein purification (**Table 2**). Due to the large discrepancy in protein expression success between the Autoinduction and IPTG expression systems, in many cases IPTG expression was the first and only expression system attempted for future expressions.

Preparation of SpyCatcher EQ. The second protein purified was SpyCatcher EQ the inactive mutant to SpyCatcher WT which lacks a catalytic glutamic acid residue.

Preparation of BL21(DE3)/pDEST14-SpyCatcher EQ strain. pDEST14-SpyCatcher EQ was extracted from a BL21(DE3)/pDEST14-SpyCatcher EQ strain using

E.Z.N.A Kit Mini-Prep (**Figure 26**). Due to the use of RNase, there is no smearing near the bottom of the gel after digestion with *EcoRI*.

Table 2. Protein purification table. Table including protein purification values found through Bradford Assay with BSA standard.

Sample Name	Total Soluble Protein After Lysis of ~ 0.5 g of Cell Pellet	Total Purified Protein From ~0.5g of Cell Pellet	Percent of Protein of Interest in Total Soluble Protein
SpyCatcher WT IPTG	14.4 mg	3.54 mg	24.5%
SpyCatcher EQ IPTG	10.0 mg	3.37 mg	33.7%
SpyTagMBP IPTG	32.3 mg	8.62 mg	26.7%
SpyCatcher WT Autoinduction	7.00 mg	0.0257 mg	0.367%
SpyTag-mEGRP-SnoopTag Autoinduction	31.8 mg	12.2 mg	38.5%

While the plasmid bands are in the reported spot for pDEST14 SpyCatcher EQ, 4061 bp, the bands were very faint in comparison to the bands of the DNA ladder. This could be the result of poor extraction, low copy number, or incomplete DNA staining, but it was good enough to confirm the presence of pDEST14-SpyCatcher EQ inside the bacteria strain, and continue on to protein expression.

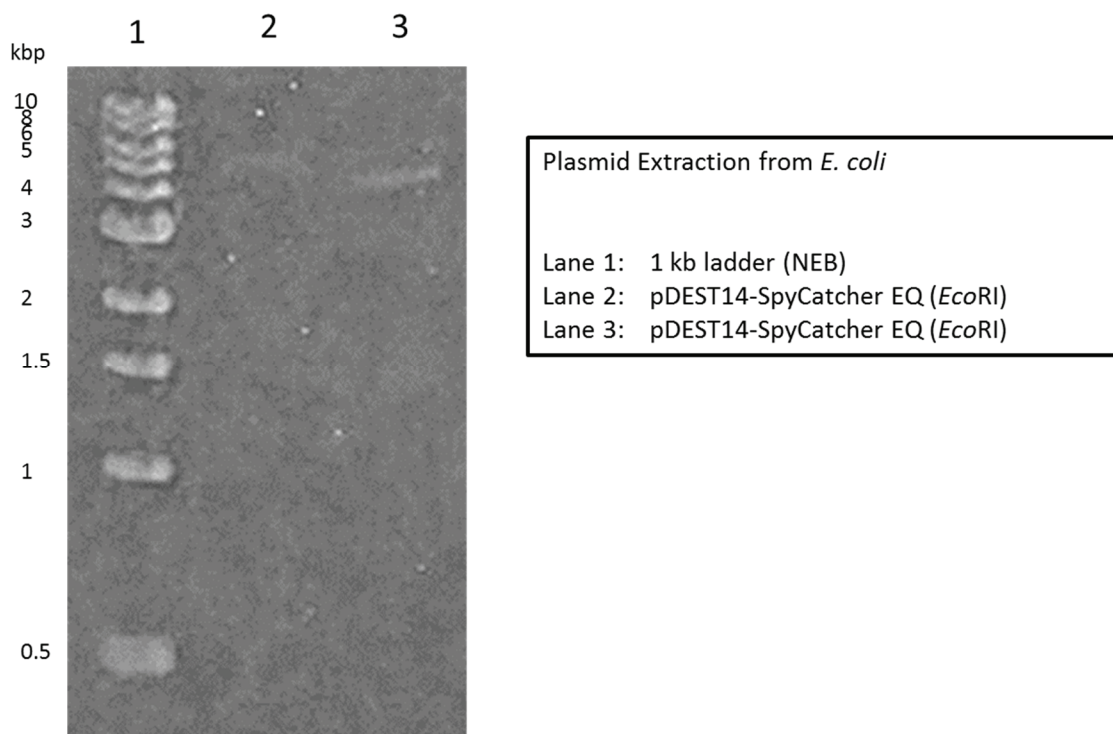


Figure 26. Electrophoresis of pDEST14-SpyCatcher-EQ on 1% agarose gel. Lane 1: 1 kb DNA Ladder (New England BioLabs®). Lanes 2 and 3: pDEST14-SpyCatcher EQ(4061 bp) digested with *Nde*I.

Expression of SpyCatcher EQ with Induction by IPTG. It took approximately 4 times longer for BL21(DE3)/pDEST14-SpyCatcher EQ than BL21(DE3)/pDEST14-SpyCatcher to reach an OD₆₀₀ of 2 after 9 hours (**Figure 24**). IPTG was then added to induce the expression of the protein resulting in 1.1143 g of bacterial cells in wet weight.

Purification of SpyCatcher EQ. SpyCatcher EQ, the inactive mutant of SpyCatcher, could be successfully purified through IPTG (**Figure 27**). After dialysis, 6 tubes containing approximately 1000 µL of 0.98 mg/mL-0.24 mg/mL SpyCatcher EQ samples were obtained. Using the same purification method as for SpyCatcher WT, an increase in the purity of SpyCatcher EQ from the soluble fraction can be achieved. It is interesting to note that in this gel is seen in the intense band of the protein of interest in

the flow through lane (lane 3). This band is likely the result of saturation of the Ni^{2+} -NTA column during the loading. Due to this loss of protein in the flow through fraction, the calculated protein yield shown in Table 2 should be slightly off of what was actually expressed.

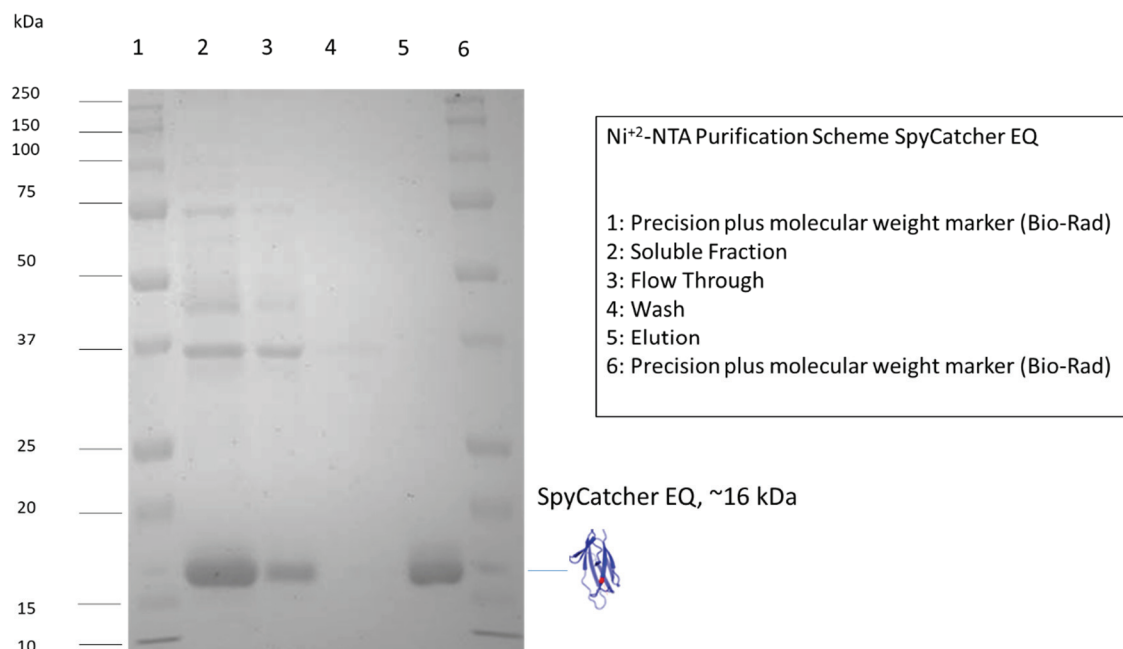


Figure 27. SDS-PAGE of each fraction during the purification of SpyCatcher EQ. Purification steps of SpyCatcher WT. Lane 1: Precision plus molecular weight marker (Bio-Rad). Lane 2: soluble fraction. Lane 3: flow through of soluble fraction. Lane 4: wash fraction. Lane 5: elution fraction. Lane 6: Precision plus molecular weight marker (Bio-Rad).

Determination of SpyCatcher EQ Expression Success. Table 2 shows the amount of purified SpyCatcher EQ. This was similar to that of SpyCatcher WT, 3.37 mg from ~ 0.5 g wet weight of BL21(DE3)/pDEST14-SpyCatcher EQ when induced by IPTG as evaluated by Bradford Assay using a BSA standard. The percentage of SpyCatcher EQ

came out to be around 33.7% of total protein in the soluble protein fraction, slightly higher than that of SpyCatcher WT.

Preparation of SnoopTag-mEGFP-SpyTag. The third protein purified was SnoopTag-mEGFP-SpyTag, fluorescently tagged SpyTag of ~34 kDa.

Preparation of BL21(DE3)/pET28a SnoopTag-mEGFP-SpyTag strain. **Figure 22**, shows the result of agarose gel electrophoresis for pET28a SnoopTag-mEGFP-SpyTag. Kit-free Mini-Prep was used to extract pET28a SnoopTag-mEGFP-SpyTag from BL21(DE3)/pET28a SnoopTag-mEGFP-SpyTag strain and digested with *NdeI* before electrophoresis. The plasmid bands found in lanes 4 and 5 agree with previously reported size of the pET28a SnoopTag-mEGFP-SpyTag (6154 bp), and were fairly intense indicating successful extraction. The smears at the bottom of the lanes were again attributed to RNA as the Mini-Prep does not employ RNase.

Expression of SnoopTag-mEGFP-SpyTag by AutoInduction. Autoinduced protein expression resulted in a large growth rate in SnoopTag-mEGFP-SpyTag even though cell densities did not get as high as with SpyCatcher T51A. After ~20 hours, OD_{600} plateaued around 10 and cells were allowed to express for 6 more hours before being removed for protein purification (**Figure 23**). This resulted in 1.971 g of *E. coli*, close to double the wet weight obtained by IPTG induction.

Purification of SnoopTag-mEGFP-SpyTag. The cells harvested after autoinduced expression were subjected to purification *via* Ni^{2+} -NTA column and a purification gel was made, (**Figure 28**). After dialysis, 11.3 mL of 1.11 mg/mL SnoopTag-mEGFP-SpyTag sample was obtained. In lane 2, the whole soluble fraction of the cell is shown. This fraction is the result of cell lysing and centrifugation, containing all soluble cellular

proteins. While many bands are present, the most intense band can be seen at ~34 kDa, exactly where the protein of interest is expected to be found. Lane 2 shows the flow through fraction during Ni²⁺-NTA purification and many bands of protein impurity, and the band density in the area of the protein of interest was significantly lower. Lane 4 shows the wash lane of the Ni²⁺-NTA purification and no protein bands were observed. Finally, lane 5 shows the eluted purified protein. In this lane, it can be clearly observed that there is no visible banding besides the band at ~34 kDa. This lack of the other visible bands that were present in the soluble protein fraction indicates the high purity of the obtained protein.

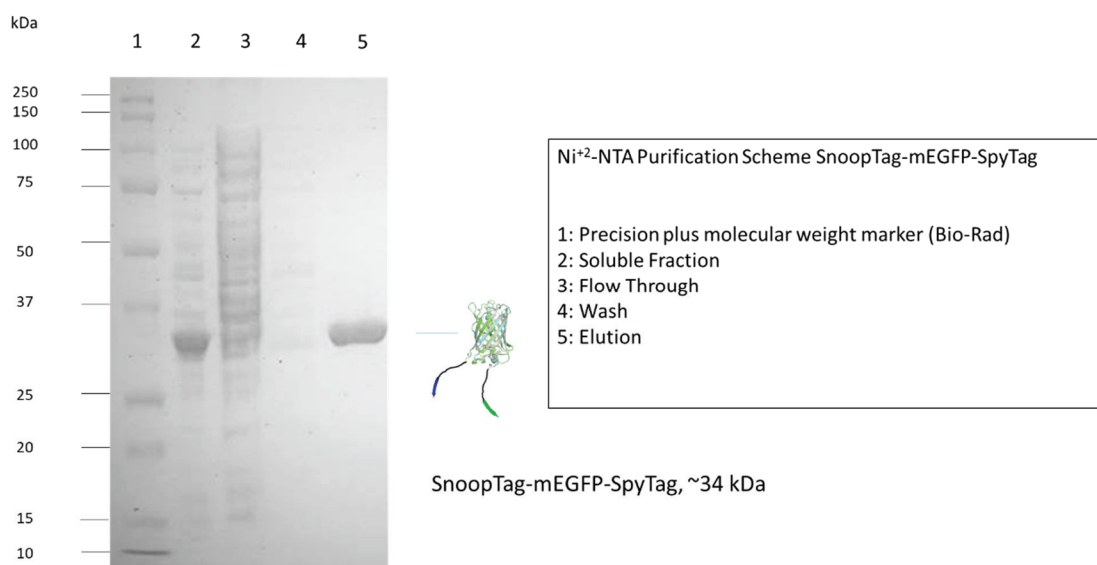


Figure 28. SDS-PAGE of each fraction during the purification of SnoopTag-mEGFP-SpyTag. Purification steps of SnoopTag-mEGFP-SpyTag. Lane 1: Precision plus molecular weight marker (Bio-Rad). Lane 2: soluble fraction. Lane 3: flow through of soluble fraction. Lane 4: wash fraction. Lane 5: elution fraction.

Determination of SnoopTag-mEGFP-SpyTag WT Expression Success. Using

Bradford Asssay with a BSA standard, a very high yield for SnoopTag-mEGFP-SpyTag

could be determined, ~12.21 mg from ~0.5 g wet weight of BL21(DE3)/pET28a SnoopTag-mEGFP-SpyTag, the highest yield achieved among the proteins purified in this work (Table 2). For this protein, autoinduction yielded an ideal result. The reason for the inconsistency observed in the cell growth between autoinduced protein expressions has yet to be determined, it was well reflected in the amount of protein that was capable of being purified. This resulted in visibly green proteins that fluoresce under blue and UV light.

Preparation of SpyTagMBP. The final protein purified was SpyTagMBP, a SpyTag which has been covalently linked to maltose binding protein for its 42 kDa size.

Preparation of BL21(DE3)/pET28a-SpyTagMBP strain. The final plasmid purified was pET28a-SpyTagMBP (**Figure 29**). After Mini-Prep of BL21(DE3)/pET28a-SpyTagMBP stain and digestion with *EcoRV* and agarose gel electrophoresis, extremely intense bands were observed in all lanes containing the Mini-Prep extraction product. Though this extraction being Mini-Prep shows characteristic RNA streaking, the singular bands observed matched exactly with the reported size of pET28a-SpyTagMBP for this digestion (6484 bp). These intense bands are indicative of a successful extraction.

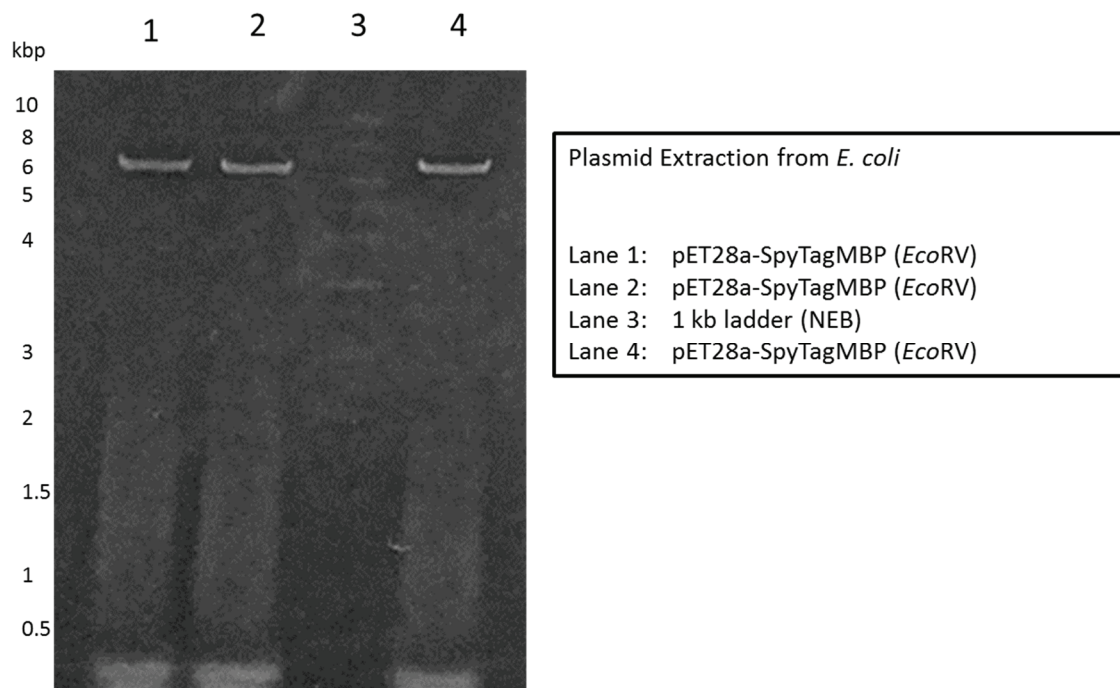


Figure 29. Electrophoresis of pET28a-SpyTagMBP on 1% agarose gel. Lane 3: 1 kb DNA Ladder (New England BioLabs®). Lanes 1, 2 and 4: pET28a-SpyTagMBP (6484 bp) digested with *EcoRV*.

Expression of SpyTagMBP with induction by IPTG. SpyTagMBP was expressed using the IPTG induction (**Figure 24**). During initial growth, it took ~3.5 hours for SpyTagMBP to get to an optical density of 1.8 making it the second fastest of the cultures that went through this expression system. The total amount of harvested bacterial cell was 1.0923 g in wet weight.

Purification of SpyTagMBP. The SpyTagMBP could be successfully purified resulting in no detectable co-purification (**Figure 30**). After dialysis, 8 tubes containing approximately 1000 μ L of 1.6 mg/mL-0.62 mg/mL SpyCatcher WT samples were obtained. One unique thing observed in this gel is that there seems to be a loss of the desired protein (~42 kDa) in each step. Even with protein being lost in wash and flow through fractions, the final purified band showed a relatively large amount of protein.

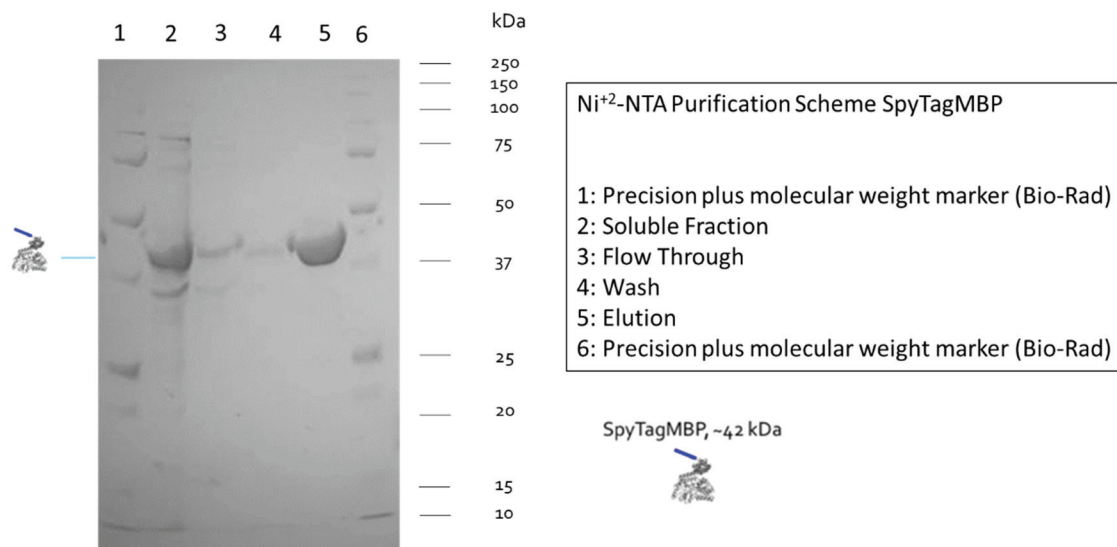


Figure 30. SDS-PAGE of each fraction during the purification of SpyTagMBP. Purification steps of SpyTagMBP. Lane 1: Precision plus molecular weight marker (Bio-Rad). Lane 2: soluble fraction. Lane 3: Flow through of soluble fraction. Lane 4: wash fraction. Lane 5: Elution Fraction. Lane 6: Precision plus molecular weight marker (Bio-Rad).

Determination of SpyTagMBP Expression Success. The yield of the SpyTag MBP expressed by IPTG induction was determined through Bradford Assay using a BSA standard. SpyTagMBP had more than twice the mass yield from ~0.5 g of wet weight BL21(DE3)/pET28a-SpyTagMBP as SpyCatcher WT and SpyCatcher EQ, 8.62 mg (Table 2). This could be caused by several things including the amino acids needed to construct each protein, or the plasmid differences in antibiotic resistances, SpyCatcher WT and SpyCatcher EQ were coded on a plasmid with ampicillin resistance while SpyTagMBP was coded on a plasmid with kanamycin resistance. Another possibility is that the mode of concentration detection, Bradford Assay with a BSA standard, is more effective with proteins that are of approximately the same size and make-up. SpyCatcher and SpyCatcher EQ are β -sheet rich and only differ by a single amino acid, SpyTagMBP

is a much larger, almost 3 times the size of the SpyCatcher's, and has a much wider variety of secondary structure.

Confirmation of Isopeptide Bond Forming Activity. The activity of SpyCatcher WT, and SpyCatcher EQ were confirmed using SDS-PAGE in conjunction with a SpyTag fused protein, SnoopTag-mEGFP-SpyTag (**Figure 31**, **Figure 32**). In lane 2, 3, and 4 of this gel, SpyCatcher WT, SpyCatcher EQ, and SnoopTag-mEGFP-SpyTag, can be observed respectively at the concentration being used in the activity tests. Lanes 5 and 6 were loaded with samples that contain each protein of the same concentrations as in lane 2, 3, and 4. The contents of each of these wells was SpyCatcher WT and SnoopTag-mEGFP-SpyTag (lane 5), and SpyCatcher EQ and SnoopTag-mEGFP-SpyTag (lane 6) that had each been incubated for 1 hour. Lane 5 shows an intense band at ~50 kDa with almost complete depletion of the SpyCatcher WT band (~16 kDa) and complete depletion of SnoopTag-mEGFP-SpyTag band (~34 kDa). The size of this new band also nearly perfectly reflects the size of the protein that would be formed from combining of these two proteins. This simple addition of the two sizes may not always be the case due to SDS-PAGE being designed for the traveling of a completely linearized protein through the gel matrix, and the addition of an isopeptide bond effectively branches the protein. In lane 6, SpyCatcher EQ (~16 kDa) can still be observed along with SnoopTag-mEGFP-SpyTag (~34 kDa) with no other bands present in the lane. The lack of any other bands indicates the lack of covalent bond formation between the two proteins.

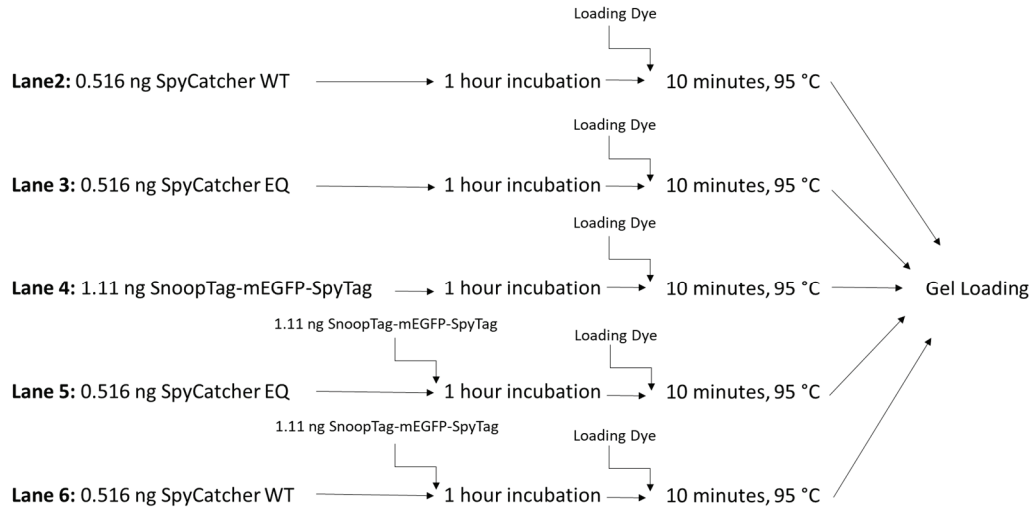


Figure 31: SpyCatcher/SpyCatcher EQ activity gel scheme. “Scheme showing sample preparation for Activity of SpyCatcher WT and SpyCatcher EQ determined on SDS-PAGE”.

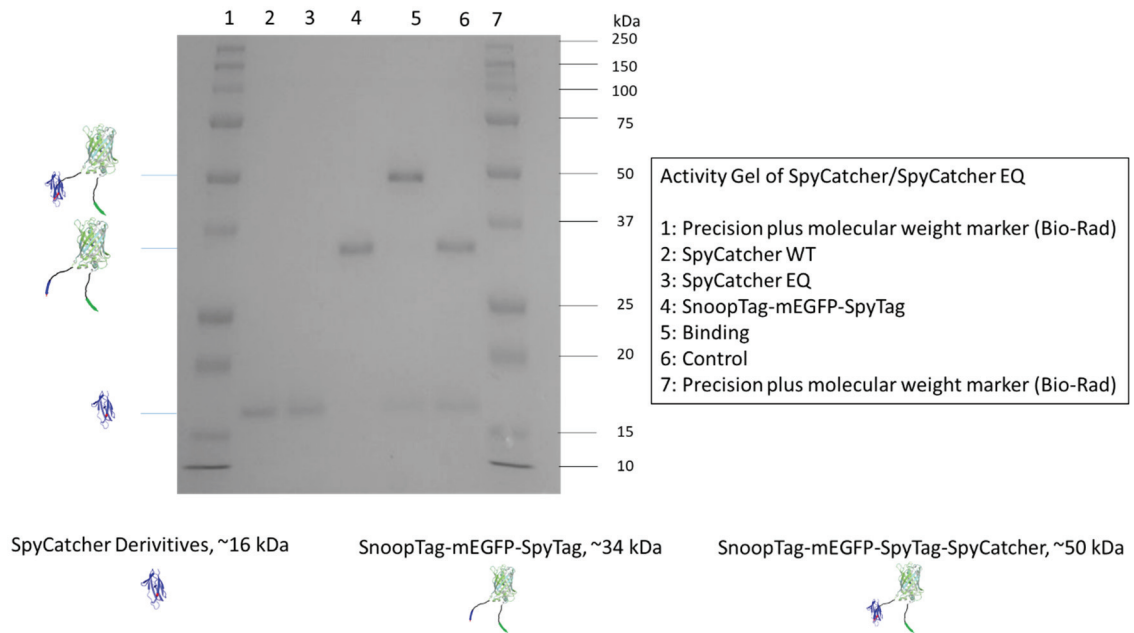


Figure 32. Activity of SpyCatcher WT and SpyCatcher EQ determined on SDS-PAGE. Lane 1: Precision plus molecular weight marker (Bio-Rad). Lane 2: SpyCatcher WT. Lane 3: SpyCatcher EQ. Lane 4: SnoopTag-mEGFP-SpyTag. Lane 5: SpyCatcher WT and SnoopTag-mEGFP-SpyTag. Lane 6: SpyCatcher EQ and SnoopTag-mEGFP-SpyTag. Lane 7 Precision plus molecular weight marker (Bio-Rad).

Fluorescence Polarization/Depolarization

Once proteins have been effectively expressed, and protein activity was confirmed, fluorescent conjugates were developed through two different paths, one of which involved the conjugation of FITC to SpyCatcher WT and SpyCatcher EQ. An alternative path was also explored which used solid-phase peptide synthesis to create a SpyTag, which was then conjugated to FITC. These two systems were to be used in fluorescence polarization/depolarization as a rapid assay to track isopeptide bond formation in real-time in homogeneous solution.

SpyCatcher-FITC Conjugates. The conjugation of FITC to SpyCatcher WT and SpyCatcher EQ lysine residues was one of the routes to fluorescence polarization/depolarization that was chosen, though it held some risk due to the isopeptide bond forming residue on SpyCatcher WT being lysine. FITC was kept at a 1:1 ratio with SpyCatcher WT to minimize this.

Confirmation of Isopeptide Bond Forming Activity between SpyTagMBP and SpyCatcher-FITC Derivatives. SDS-PAGE was used to check for activity of FITC-labeled proteins once the conjugation was complete (**Figure 33**, **Figure 34**). The experiment followed the same format as previous ones with the three parts being shown separately in lanes 2, 3, and 4, and lanes 5 and 6 being combinations of SpyTagMBP with either SpyCatcher WT-FITC (lane 5) or SpyCatcher EQ-FITC (lane 6) that were incubated for one hour. The gel shows exactly what we expected for the band retardation of SpyTagMBP in the lane containing SpyCatcher WT-FITC and no change in the lane with SpyCatcher EQ-FITC. When comparing lane 5 before and after staining gels, a fluorescent band is present in the place of SpyCatcher WT-FITC that is not concentrated

enough to be clearly observed through normal SDS-PAGE staining. This could be due to SpyCatcher WT-FITC that was inactive due to loss of its fold during freeze thaw cycles before the samples were ever combined for binding, and that will be explored more.

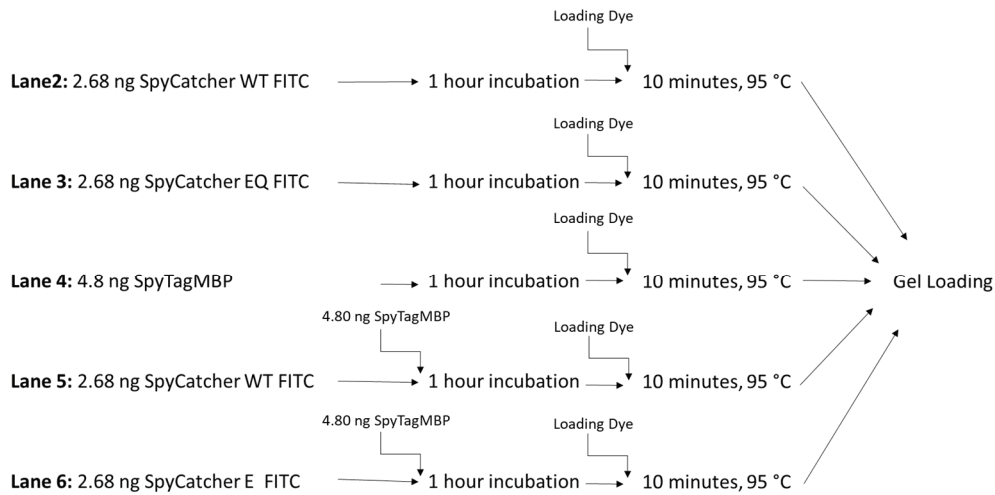


Figure 33. Scheme of isopeptide bond formation activity measurement. Scheme showing sample preparation for “SDS-PAGE showing SpyTagMBP, SpyCatcher-FITC derivative activity”.

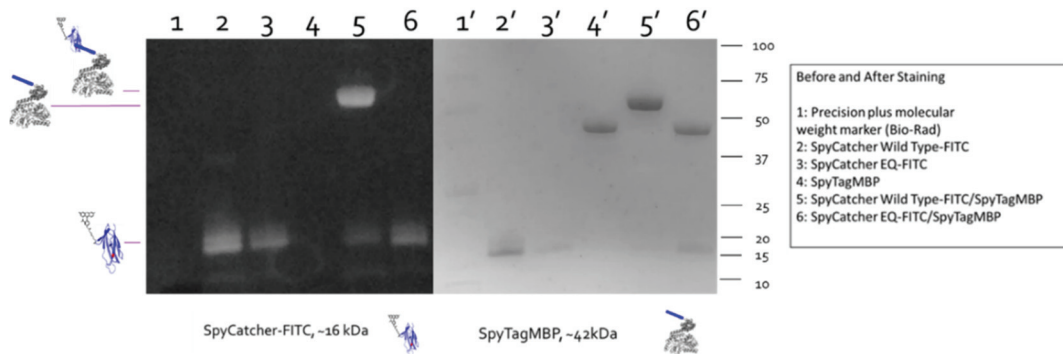


Figure 34. SDS-PAGE showing SpyTagMBP, SpyCatcher-FITC derivative activity before (right) and after (left) staining. Lane 1: Precision plus molecular weight marker (Bio-Rad). Lane 2: SpyCatcher WT-FITC. Lane 3: SpyCatcher EQ-FITC. Lane 4: SpyTagMBP. Lane 5: SpyCatcher WT-FITC and SpyTagMBP. Lane 6: SpyCatcher EQ-FITC and SpyTagMBP.

A concentration dependence of SpyTagMBP on isopeptide bond formation activity was studied with constant SpyCatcher WT-FITC (**Figure 35**, **Figure 36**). The concentration of SpyTagMBP increase in molar equivalence from lane 2 to 7. It can be clearly seen that both SpyTagMBP, and SpyCatcher WT-FITC are completely consumed. Several different forms of folded and unfolded complexes between SpyCatcher WT-FITC and SpyTagMBP can be seen and all of them reflect consumption of the original two pieces.

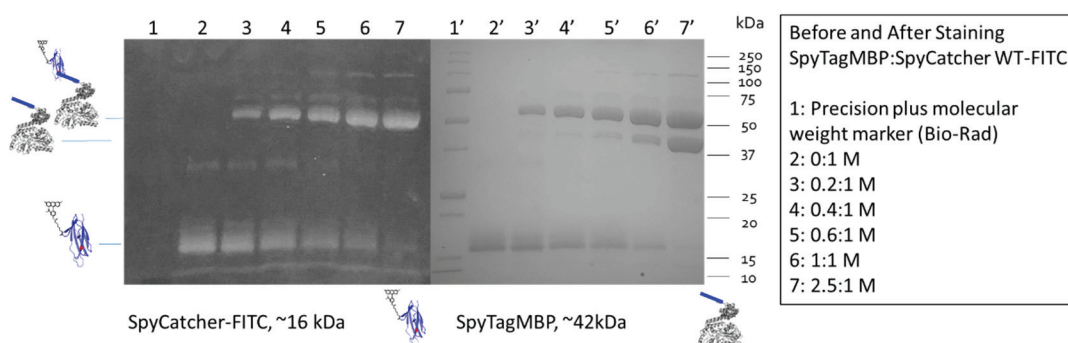


Figure 35. Concentration dependence of SpyTagMBP on isopeptide bond forming activity using SDS-PAGE before (left) and after (right) staining. Lane 1: Precision plus molecular weight marker (Bio-Rad). Lane 2-7: 0:1, 0.2:1, 0.4:1, 0.6:1, 1:1, 2.5:1 in mole equivalence of SpyTagMBP to SpyCatcher WT-FITC.

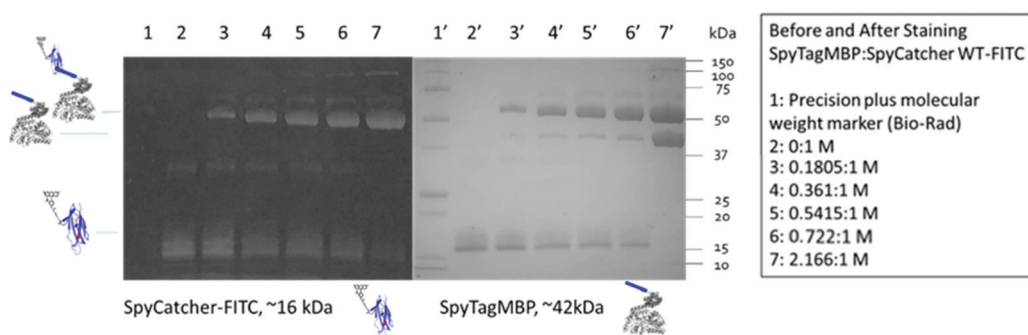


Figure 36. Concentration dependence of SpyTagMBP using SDS-PAGE for comparison with mP before (left) and after (right). Lane 1: Precision plus molecular weight marker (Bio-Rad). Lanes 2-7: 0:1, 0.1805:1, 0.361:1, 0.5415:1, 0.722:1, and 2.166:1 in mole equivalence of SpyTagMBP to SpyCatcher WT-FITC.

Fluorescence Polarization Depolarization Using SpyTagMBP and SpyCatcher-FITC Conjugates. Fluorescence polarization/depolarization measurement was employed to further study the isopeptide bond forming activity of SpyCatcher WT-FITC, SpyCatcher EQ-FITC, and SpyTagMBP. Raw Data can be found in Appnedix III.

Concentration Dependence of SpyTagMBP. **Figure 37** shows the dependence of mP (millipolarization) on the concentration of SpyTagMBP after two hours of incubation. It is, however, interesting to note that as molar equivalence of SpyTagMBP increased, SpyCatcher WT-FITC showed a rapid increase in mP that leveled out as it became saturated, while SpyCatcher EQ-FITC on the other hand had a much lower change in the presence and absence of SpyTagMBP. Unfortunately, the beginning mP values for SpyCatcher EQ-FITC and SpyCatcher WT-FITC are not the same, which makes comparing them difficult. It is possible that the difference in starting mP between SpyCatcher WT-FITC and SpyCatcher EQ-FITC is due to unequal degree of conjugation with FITC resulting in larger SpyCatcher EQ-FITC molecules that depolarize light to a lower extent.

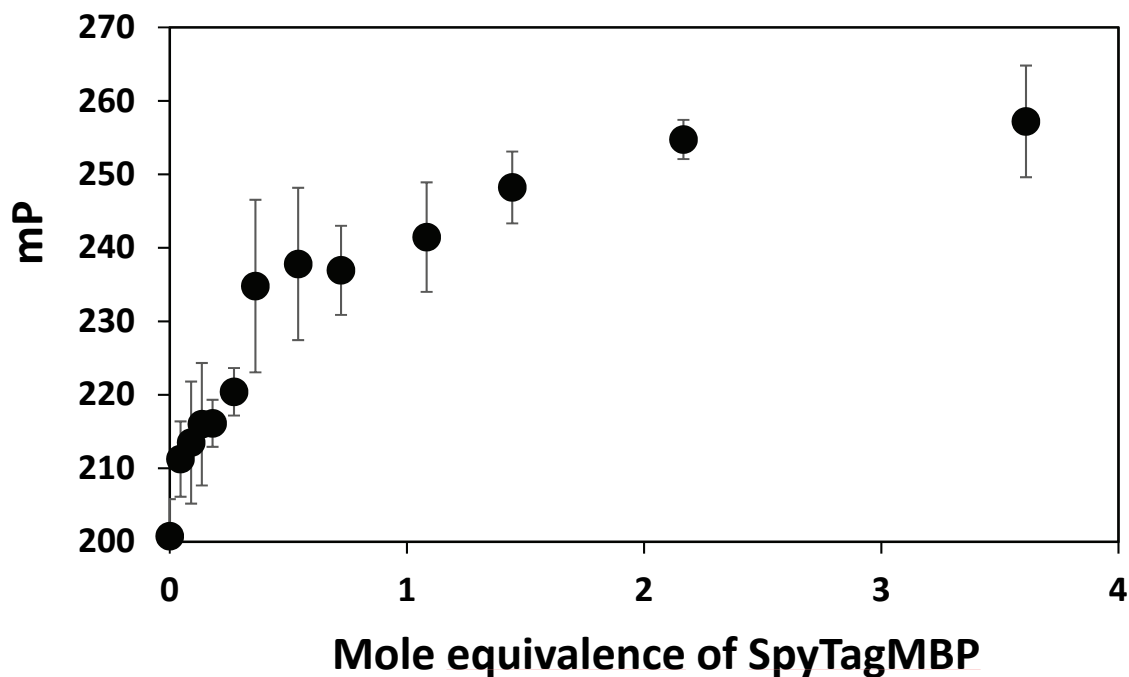


Figure 37. Concentration dependence of SpyTagMBP on mP. Showing the change in mP of SpyCatcher WT-FITC and SpyCatcher EQ-FITC in the presence of different molar equivalence of SpyTagMBP. SpyCatcher EQ results can be found in Appendix B-1. Error bars show plus or minus one standard deviation of four runs.

Correlation between Fluorescence Polarization/Depolarization and Band

Intensity Ratio. Using ImageJ, a ratio between intensity for SpyTagMBP-SpyCatcher WT-FITC complex and SpyCatcher WT-FITC were taken from **Figure 36 (Figure 38)** and compared to mP values of the same molar equivalence (**Figure 39**). ImageJ analysis showed a linear increase in SpyTagMBP-SpyCatcher WT-FITC complex as SpyCatcher WT-FITC decreased linearly.

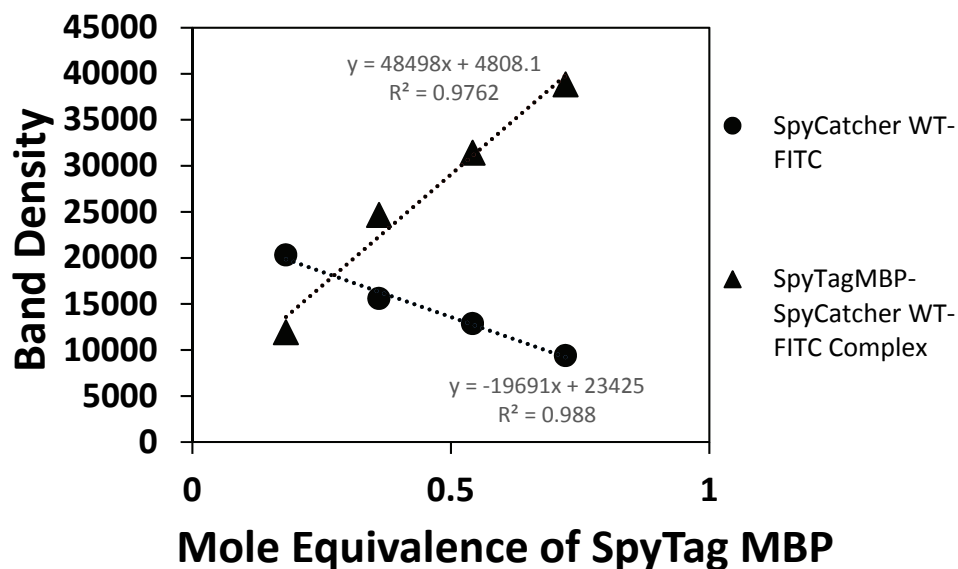


Figure 38. Molar equivalence on SDS-PAGE using ImageJ. Band determined through ImageJ of SDS-PAGE band in “Concentration dependence of SpyTagMBP using SDS-PAGE for comparison with mP before (left) and after (right)”. Circle marks represent SpyTagMBP-SpyCatcher WT-FITC Complex, and squares represent SpyCatcher WT-FITC. Table of Values can be found in Appendix C.

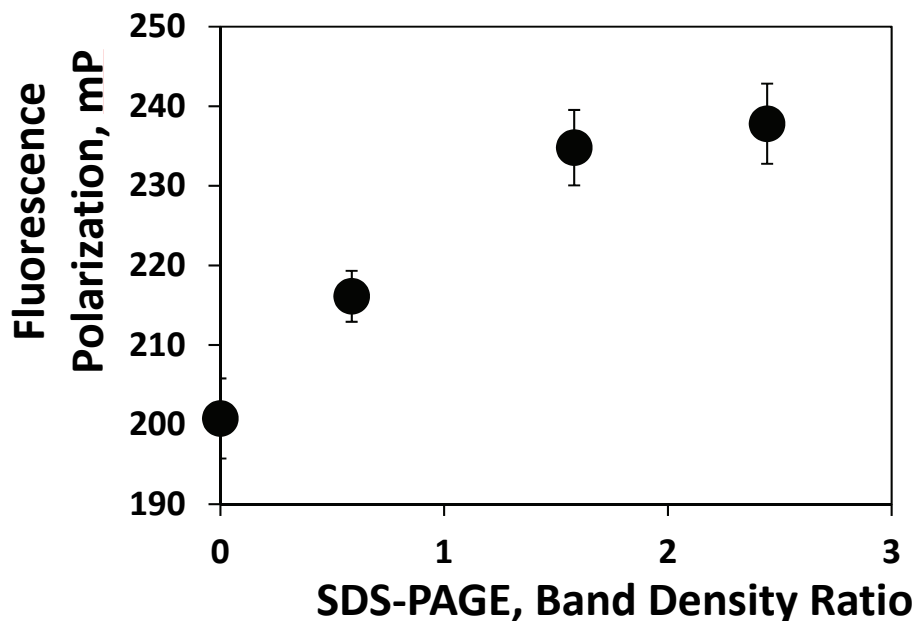


Figure 39: Band intensity ratio vs mP for different SpyTagMBP molar equivalence. The plot showing the correlation between mP and band intensity ratio from SDS-PAGE. Error bars show plus or minus one standard deviation of four runs. Full range of points can be found in Appendix B-2.

Kinetic Study. The molar equivalence ratio of 0.51 was chosen due to its location near the center of upward trend in the concentration dependence study (**Figure 37**). The mP value of SpyCatcher WT-FITC is around 200, while the first reading during the kinetic study recorded at ~313 due to the time lag between experiment set up and data acquisition (**Figure 40**). A rapid rise in mP can be seen very early on which levels out to a slow rising plateau. The leveling point was determined after an hour due to the mP reaching the mP value recorded after two hours at just a single hour. There is some fluctuation that occurs during the plateau of this curve which could be due to a small samples size, or from slight differences in SpyCatcher WT or SpyTag MBP populations.

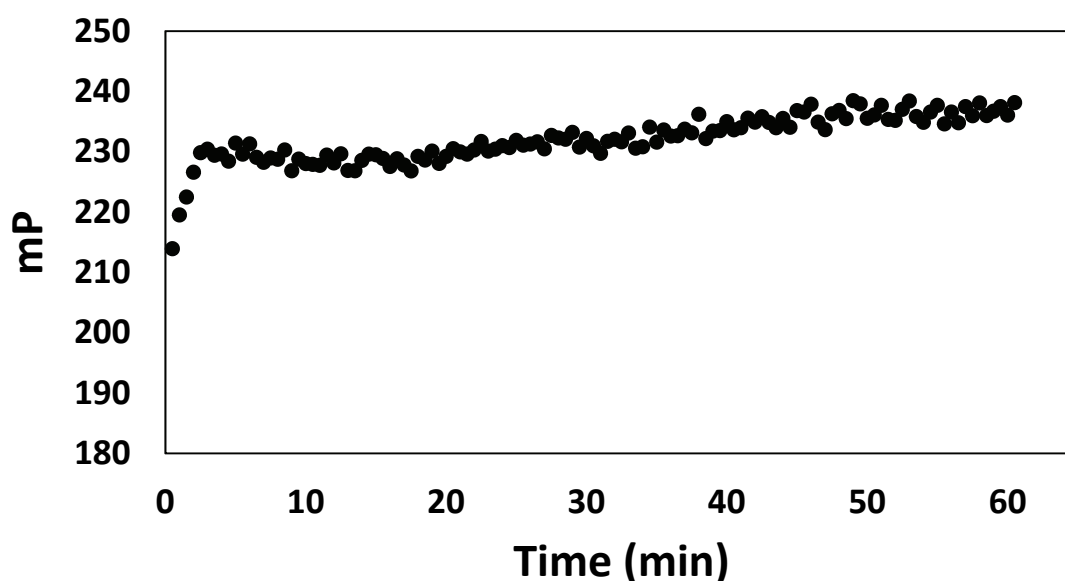


Figure 40. Kinetic study. Fluorescence polarization/depolarization study of 0.51 M equivalence of SpyTagMBP over one hour. Graph with error bars and separate graphs of all four runs can be found in Appendix B-2-Appendix B-7.

SpyTag-FITC Conjugate. Another route to fluorescence polarization discussed involves a solid-phase peptide synthesized SpyTag that was conjugated to FITC through an N-terminal linker, β -alanine.

Confirmation of FITC Coupling Completion. To confirm the conjugation of FITC to the β -alanine of the synthesized SpyTag, a Kaiser Test was used (**Figure 41**). In a Kaiser Test, the presence of a primary amine results in a deep blue color change. In the far left test tube, non-protected PEG-rink amide resin shows a deep blue color from the presence of its free amines. The middle tube holds PEG-rink amide resin after the peptide synthesis and subsequent deprotection of SpyTag. A deep blue can be seen here too as the deprotected β -alanine on the N-terminal reacts with the ninhydrin. The final test tube contains PEG-rink amide resin, and the synthesized SpyTag that has undergone a coupling reaction with FITC. This test tube has no blue color at all, showing a lack of primary amines and indicating a complete coupling of the β -alanine residues to a FITC molecule.

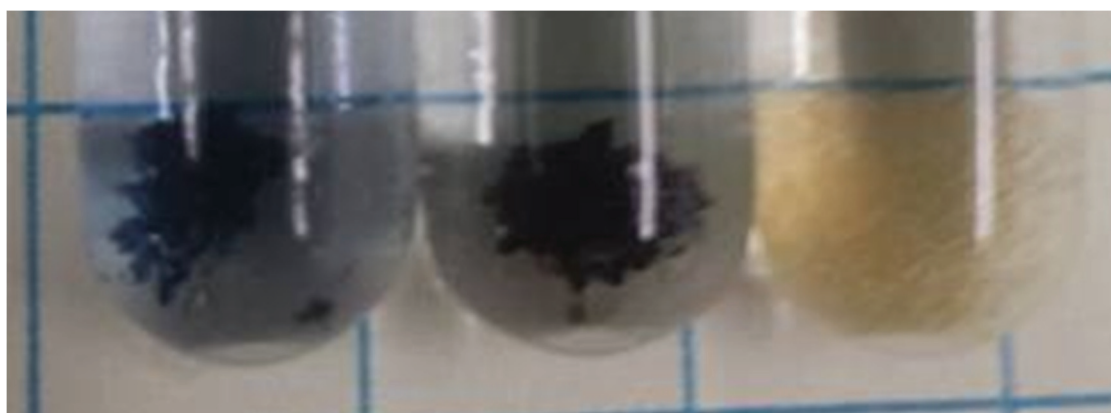


Figure 41. Kaiser test. Shows the progression of PEG-rink amide resin through Kaiser Tests from just resin (left), to resin and peptide (middle), to resin, peptide, and FITC (right).

Confirmation of Isopeptide Bond Forming Activity Between SpyTag-FITC and SpyCatcher Derivatives. After Coupling with FITC and cleavage from the PEG-rink amide resin, the activity of the fluorescently labeled SpyTag was tested against SpyCatcher WT and SpyCatcher EQ with SDS-PAGE after an hour long incubation of each sample (**Figure 42**). Unfortunately, once stained, FITC no longer has fluorescent properties, so gel images are taken before and after staining. Due to the inability to view the bands simultaneously, the before staining gel will be discussed first. Lane 4 can be observed as the control lane, containing only SpyTag-FITC. This band can be seen up near the dye front as SpyTag-FITC is only 13 residues long. In lane 5, the lane containing both SpyCatcher WT and SpyTag-FITC, there is large movement of the band toward a high molecular weight region. Interestingly, this shift is indicative of what would be expected for a protein of a much larger size than that of just the SpyCatcher, SpyTag-FITC complex, and this point will be discussed further later. Finally, lane 6, the lane containing SpyCatcher EQ and SpyTag FITC, shows no shift of the fluorescent band derived from SpyTag-FITC. This lack of shift of the fluorescent band demonstrates no covalent bond formation taking place between SpyCatcher EQ and SpyTag-FITC. In the stained image, the band for SpyCatcher WT and SpyCatcher EQ can be seen, and they support the conclusions drawn from the before staining image. Comparing lane 5 of the stained and non-stained gel, it does seem that neither SpyCatcher WT nor our SpyTag-FITC was consumed. The lack of consumption of SpyCatcher WT or SpyTag-FITC, and the previously tested activity for SpyCatcher WT indicates that there is some form of inactive peptide in our SpyTag-FITC sample which still has fluorescence that could interfere with fluorescent polarization in too large of a presence.

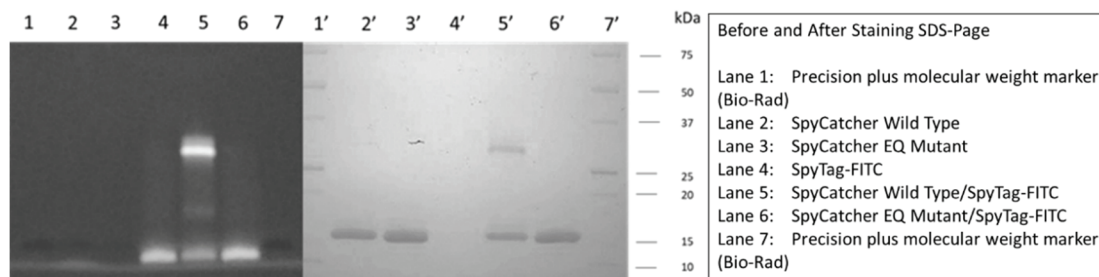


Figure 42. SDS-PAGE SpyTag-FITC activity before (left) and after (right) staining. Lane 1: Precision plus molecular weight marker (Bio-Rad).. Lane 2: SpyCatcher WT. Lane 3: SpyCatcher EQ. Lane 4: SpyTag-FITC. Lane 5: SpyCatcher WT and SpyTag-FITC. Lane 6: SpyCatcher EQ and SpyTag-FITC. Lane 7: Precision plus molecular weight marker (Bio-Rad).

In order to study why the band movement upon isopeptide bond formation with SpyCatcher WT and SpyTag-FITC was so much larger than anticipated, a Blue Native PAGE was performed to see if the stability gained through isopeptide bond formation allowed for SpyCatcher to keep its fold and not travel linearly through the gel (**Figure 43**). Blue Native PAGE works through the premise of not using SDS, 2-mercaptoethanol, or boiling to cause protein denaturation. Instead, protein samples were mixed with a negatively charged dye (coomassie brilliant blue) in order give a negative charge to the protein and cause movement to the anode during electrophoresis. The before staining gel seems identical to the inverse of the SDS-PAGE gel, this is due to the surface area available to negative charges to bind. In the stained gel, lane 4 shows a much smaller change between SpyCatcher WT and SpyCatcher WT, SpyTag-FITC complex bands, and interestingly also shows resolution between SpyCatcher WT and SpyCatcher EQ from the difference of a singular charge. The smaller change observed in the gel between the folded structures agrees with the hypothesis that the large band

reduction observed in SDS-PAGE was due to the complex not unfolding upon traditional SDS-PAGE stressors.

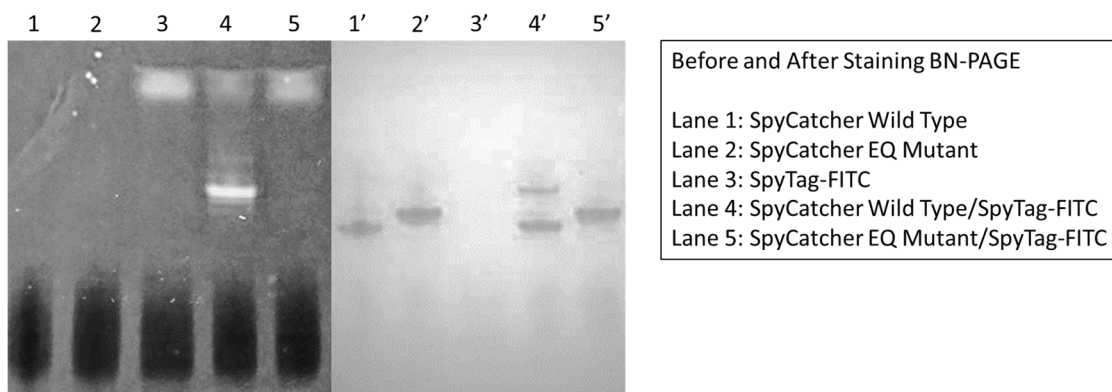


Figure 43. BN-PAGE SpyTag-FITC activity before (left) and after (right) staining. Lane 1: Precision plus molecular weight marker (Bio-Rad). Lane 2: SpyCatcher WT. Lane 3: SpyCatcher EQ. Lane 4: SpyTag-FITC. Lane 5: SpyCatcher WT and SpyTag-FITC. Lane 6: SpyCatcher EQ and SpyTag-FITC. Lane 7: Precision plus molecular weight marker (Bio-Rad).

Purity of Synthesized SpyTag-FITC Conjugate. The peptide was analyzed by MALDI-TOF MS in collaboration with Professor Keykavous Parang of Chapman University. Upon receiving the MALDI-TOF MS data (**Figure 44**), it became clear that there was a large amount of impurity in the sample. Our peptide of interest was a lower product at about 1930 m/z. The dominant product matched our peptide of interest without an aspartic acid residue, which would explain the inactivity of a large portion of our peptide. Purification through reverse phase flash chromatography was attempted but was unsuccessful. Purification of the peptide by preparation HPLC would be an option to pursue further.

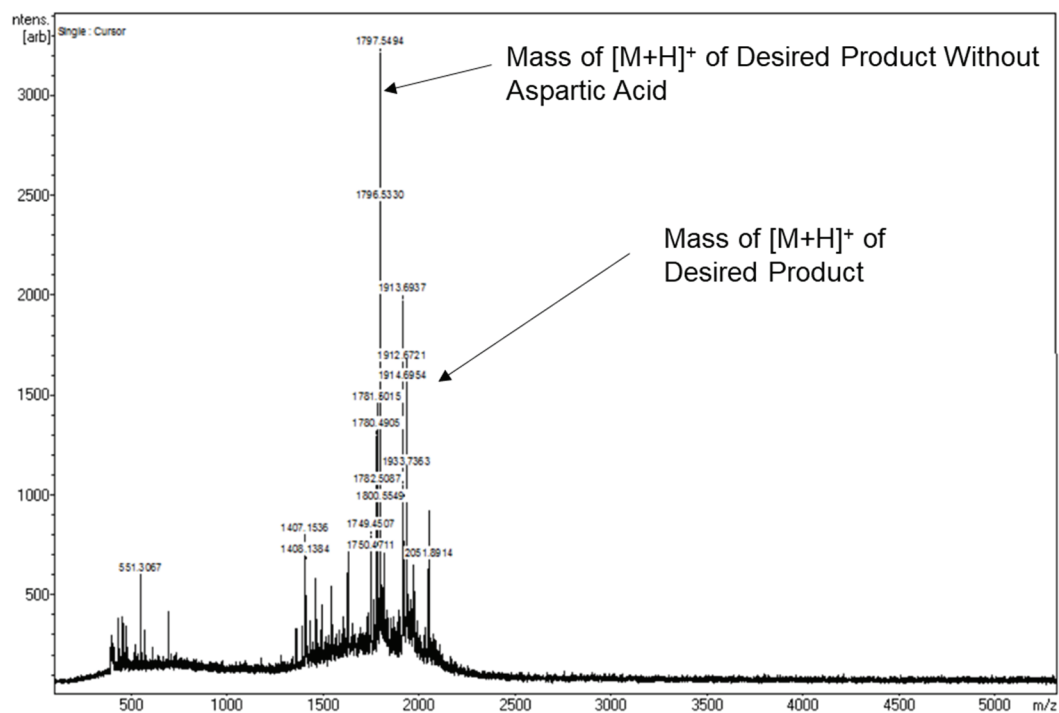


Figure 44. MALDI analysis. MALDI analysis of fluorescently coupled peptide.

CONCLUSION

The SpyCatcher/SpyTag intramolecular autocatalytic isopeptide bond forming system has the potential to be a molecular recognition element effective for detection of low abundant biomarker proteins. SpyCatcher WT, SpyCatcher EQ, SnoopTag-mEGFP-SpyTag, and SpyTagMBP were expressed in order to develop a rapid, homogenous assay for investigation into these isopeptide bond forming systems. The activity of SpyCatcher WT and SpyCatcher EQ was confirmed using SnoopTag-mEGFP-SpyTag before they were conjugated to FITC. Once conjugated, SpyCatcher WT-FITC and SpyCatcher EQ-FITC were tested for activity once more using SpyTagMBP. Fluorescence polarization/depolarization was then used on this system to monitor the dependence of mP on SpyTagMBP concentration, and their interactions in real time. Another route was also tested with a solid-phase peptide synthesized SpyTag-FITC, but more purification steps were needed before fluorescence polarization/depolarization could be attempted. Fluorescence polarization/depolarization showed overlap linearity when compared to SDS-PAGE, the current gold standard for tracking interactions, at lower SpyTagMBP concentrations. Fluorescence polarization/depolarization was also able to track real time kinetic interaction between SpyCatcher and Spytag, though a control is still needed to prove validity. With these breakthroughs, we hope that with a few more experiments validating these preliminary results, fluorescence polarization/depolarization can become a new method of rapidly screening possible isopeptide bonding partners for use in tracking low abundant biomarkers.

REFERENCES

- (1) Terpe K. Overview of tag protein fusions: from molecular and biochemical fundamentals to commercial systems *Appl. Microbiol. Biotechnol.* **2003**, 60, 523-533
- (2) Evans, T., Xu, M., Pradhan, S., PROTEIN SPLICING ELEMENTS AND PLANTS: From Transgene Containment to Protein Purification *An. Rev. Plant Biol.* **2005**, 53, 375-392
- (3) Popp, M., Antos, J., Grotenbreg, G., et al. Sortagging: a versatile method for protein labeling *Nat. Chem. Biol.* **2007** 3, 707-708
- (4) Zakeri, B. Peptide targeting by spontaneous isopeptide bond formation. DPhil. University of Oxford, 2011
- (5) Qiagen. QIAexpress(R) Detection and Assay Handbook. **2002**, 3, 1-103. Ref Type: Pamphlet
- (6) Depalma, A., Keeping Tabs on Polyhistidine Tags *Gen. Eng. Biotechnol.* **2016**, 36
- (7) Tessema, M., Simons, P., Cimino, D. Glutathione-S-Transferase-Green Fluorescent Protein Fusion Protein Reveals Slow Dissociation from High Site Density Beads and Measures Free GSH Cytometry A 2006, 69, 326-334
- (8) Sandra, H., Speicher, D. Purification of Proteins Fused to Glutathione S-Transferase *Methods Mol Biol* **2011**, 681, 259–280.
- (9) Lebendiker, M., Danieli, T. Purification of Proteins Fused to Maltose-Binding Protein *Methods Mol. Biol.* **2011**, 681, 281-293.
- (10) Walker, I. H., Hsieh, P., Riggs, P. D. Mutations in maltose-binding protein that alter affinity and solubility properties. *Appl. Microbiol. Biotechnol.*, 2010, 88, 187–197.
- (11) Grodzki, A.C., Berenstein, E. Antibody purification: affinity chromatography – protein A and protein G Sepharose. *Methods Mol. Biol.* **2010**, 588, 33-41
- (12) Absolute Antibody. Other Antibody Interactions
<http://absoluteantibody.com/antibody-resources/antibody-overview/other-antibody-interactions/> (accessed May 13, 2018).
- (13) Green, NM. "Avidin". *Advances in protein chemistry.* 1975, 29, 85–133.
- (14) Rybak, J.-N., Scheurer, S. B., Neri, D. and Elia, G. Purification of biotinylated proteins on streptavidin resin: A protocol for quantitative elution. *Proteomics* **2004**, 4, 2296–2299.

- (15) Yee, C., Thompson, J., et al. Melanocyte Destruction after Antigen-Specific Immunotherapy of Melanoma *J. Exp Med* **2000**, 192,1637-1644
- (16) Resch-Genger, U., Grabolle, M., et al. Quantum dots versus organic dyes as fluorescent labels *Nat. Methods* **2008**, 5, 763–775
- (17) Houk, K. N., Leach, A. G., Kim, S. P. and Zhang, X. Binding Affinities of Host–Guest, Protein–Ligand, and Protein–Transition-State Complexes. *Angew. Chem. Int. Ed.*, **2003**, 42, 4872–4897.
- (18) Luo, Y.R. Handbook of Bond Dissociation Energies in Organic Compounds. 2003 Boca Raton, CRC Press.
- (19) Kolšek, K, Aponte-Santamaría, C, Gräter, F. Accessibility explains preferred thiol disulfide isomerization in a protein domain. *Sci Rep.* **2017**, 7, 9858.
- (20) Voet, D., Voet, J. G., Pratt, C. W. Fundamentals of biochemistry: Life at the molecular level. **2008** Hoboken, NJ: Wiley.
- (21) Dawson, P.E., Muier, T. W., Clark-Lewish, I., Kent, S.B., Synthesis of proteins by native chemical ligation *Science* **1994**, 4, 266, 776-779.
- (22) Pickart, C.M., Eddins, M.J. Ubiquitin: structures, functions, mechanisms. *Biochim et Biophys Acta.* **2004**, 1695 1–3, 55–72.
- (23) Stieren, E.S., El Ayadi, A., Xiao, Y., et al. Ubiquilin-1 is a molecular chaperone for the amyloid precursor protein *J. Biol Chem.* **2011**, 286, 35689–98.
- (24) Safren, N., El Ayadi, A., Chang, L., et al. Ubiquilin-1 overexpression increases the lifespan and delays accumulation of Huntingtin aggregates in the R6/2 mouse model of Huntington's disease. *PLoS* **2014** 27, 9
- (25) Wang, Y., Lu, J., Zhao, X., et al. Prognostic significance of Ubiquilin1 expression in invasive breast cancer *Cancer Biomark.* **2015**, 15, 635-43.
- (26) Arias-Vásquez, A., de Lau, L., Pardo, L., Liu, F., et al. Relationship of the Ubiquilin 1 gene with Alzheimer's and Parkinson's disease and cognitive function. *Neurosci. Lett.* **2007**, 424, 1-5.
- (27) Bakker, E.N., Pistea, A., VanBavel, E. Translutaminases in vascular biology: relevance for cascular remodeling and atherosclerosis *J. Vasc. Res.* **2008**, 45, 271-278
- (28) Zhu, Y., Rinzema, A., Tramper, J., et al. *Appl Microbiol Biotechnol* **1995**, 44, 277.

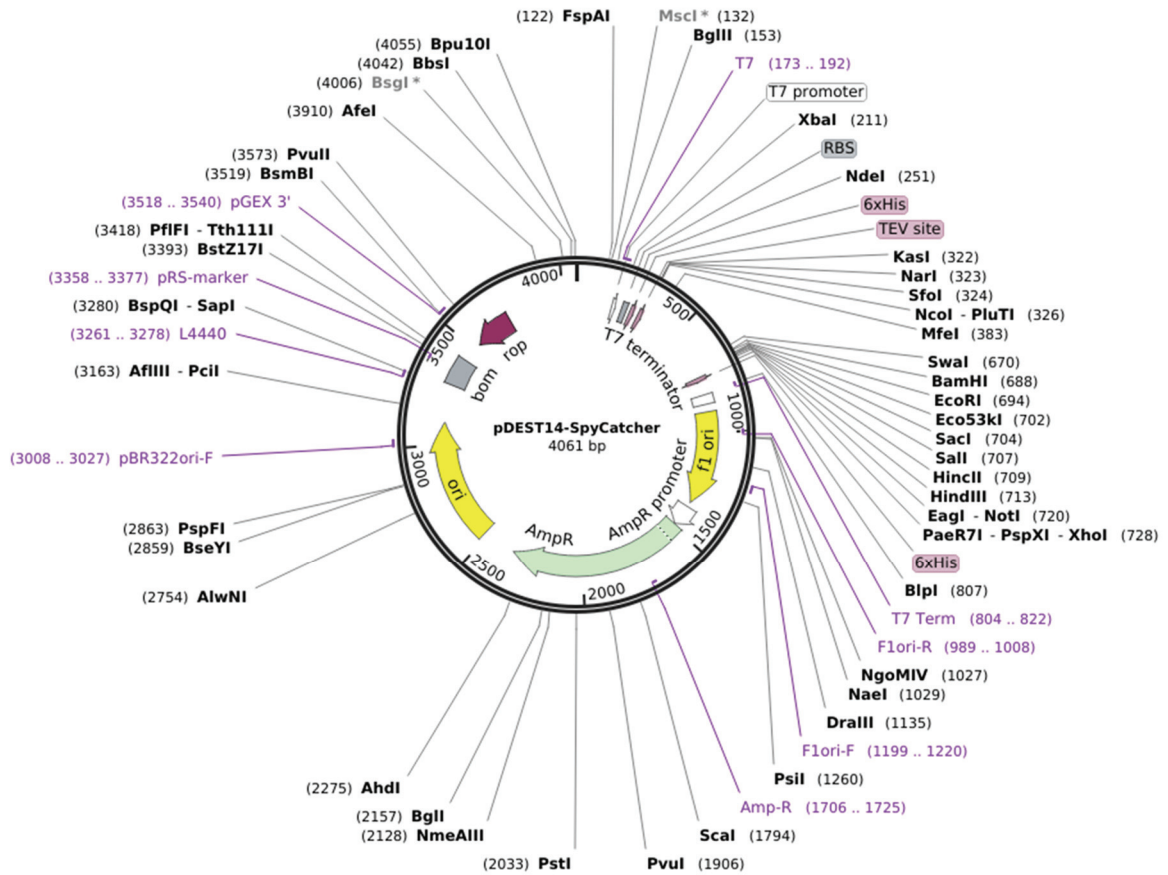
- (29) Popa, M. P., McKelvey, T. A., Hempel, J., & Hendrix, R. W. Bacteriophage HK97 structure: wholesale covalent cross-linking between the major head shell subunits. *J. Virol* **1991**, 65, 3227–3237.
- (30) Wikoff, W., Liljas, L., et al. Topologically Linked Protein Rings in the Bacteriophage HK97 Capsid *Science* **2000**, 2129-2133
- (31) Wang, B., Xiao, S., Edwards, S., Grater F. Isopeptide Bonds Mechanically Stabilize Spy0128 in Bacterial Pili *Biophys J* **2013** 104, 2051-2057
- (32) Zakeri, B., Fierer, J., Celik, E., et al. Peptide tag forming a rapid covalent bond to a protein, through engineering a bacterial adhesion *Proc. Natl. Acad. Sci.* **2012**, 109, E690-E697.
- (33) Mora M., Bensi, G., Capo S., et al. Group A *Streptococcus* produce pilus-like structures containing protective antigens and Lancefield T antigens **2005**, 102, 15641-15646
- (34) Kang, H.J., Baker, E.N. Intramolecular isopeptide bonds: protein crosslinks built for stress? *Trends Biochem Sci.* **2011**, 36, 229-37.
- (35) Alegre-Cebollada, J., Perez-Jimenez, R., Kosuri, P., Fernandez, J.M. *J Biol Chem.* **2010** 18;285(25):18961-6. Single-molecule force spectroscopy approach to enzyme catalysis.
- (36) Ghosh, I., Hamilton, A., Regan, L. Antiparallel Leucine Zipper-Directed Protein Reassembly: Application to the Green Fluorescent Protein *J. Am. Chem. Soc.*, **2000**, 122, 5658–5659
- (37) Fierer, J., Veggiana, G., Howarth, M. SpyLigase peptide-peptide ligation polymerizes affibodies to enhance magnetic cancer cell capture *Proc. Natl. Acad. Sci.* 2014, 111, E1176-E1181.
- (38) Keeble, A.H., Banerjee, A., Reddington, S.C., et al. Evolving accelerated amidation by SpyTag/SpyCatcher to analyze membrane dynamics. *Angew Chem Int Ed Engl.* **2017**
- (39) Siegmund V, Piater B, Zakeri B, et al. Spontaneous Isopeptide Bond Formation as a Powerful Tool for Engineering Site-Specific Antibody-Drug *Conj. Sci. Rep.* **2016**, 6, 39291.
- (40) Schoene C, Fierer JO, Bennett SP, Howarth M. SpyTag/SpyCatcher Cyclization Confers Resilience to Boiling on a Mesophilic Enzyme. *Angew. Chem. Int. Ed.* **2014**, 53, 6101-6104
- (41) Kumar, V., Sahal, D. Genetic Engineering. *Ullmanns Encyclopedia of Industrial Chemistry* Wiley: New York, **2014**, 1-79.

- (42) Lea, W. A., & Simeonov, A. Fluorescence Polarization Assays in Small Molecule Screening. *Expert Opin on Drug Discov.* **2011**, 6, 17–32.
- (43) Omega bio-tek Innovations in nuclei acid isolation E.A.N.A Plasmid DNA mini Kit I Product Manual **2017**
- (44) Fox, B., Blommel, P. Autoinduction of Protein Expression. *Curr. Protoc. Protein Sci.* **2009**, 5, 5.23.
- (45) Abbkine PurKine™ His-Tag Ni-NTA Resin Products Review <https://www.abbkine.com/purkine-his-tag-ni-nta-resin-products-review/> (accessed May 13, 2018).
- (46) Wittig, I., Braun, H., Schagger, H. Blue native PAGE *Nature Protocols* **2006**, 1, 418-428.
- (47) MILIPORE SIGMA Solid-phase Synthesis <https://www.sigmaaldrich.com/life-science/custom-oligos/custom-peptides/learning-center/solid-phase-synthesis.html> (accessed May 13, 2018).
- (48) SIGMA-ALDRICH Kaiser test kit Product Information <https://www.sigmaaldrich.com/content/dam/sigma-aldrich/docs/Sigma-Aldrich/Datasheet/1/60017dat.pdf> (accessed May 13, 2018).

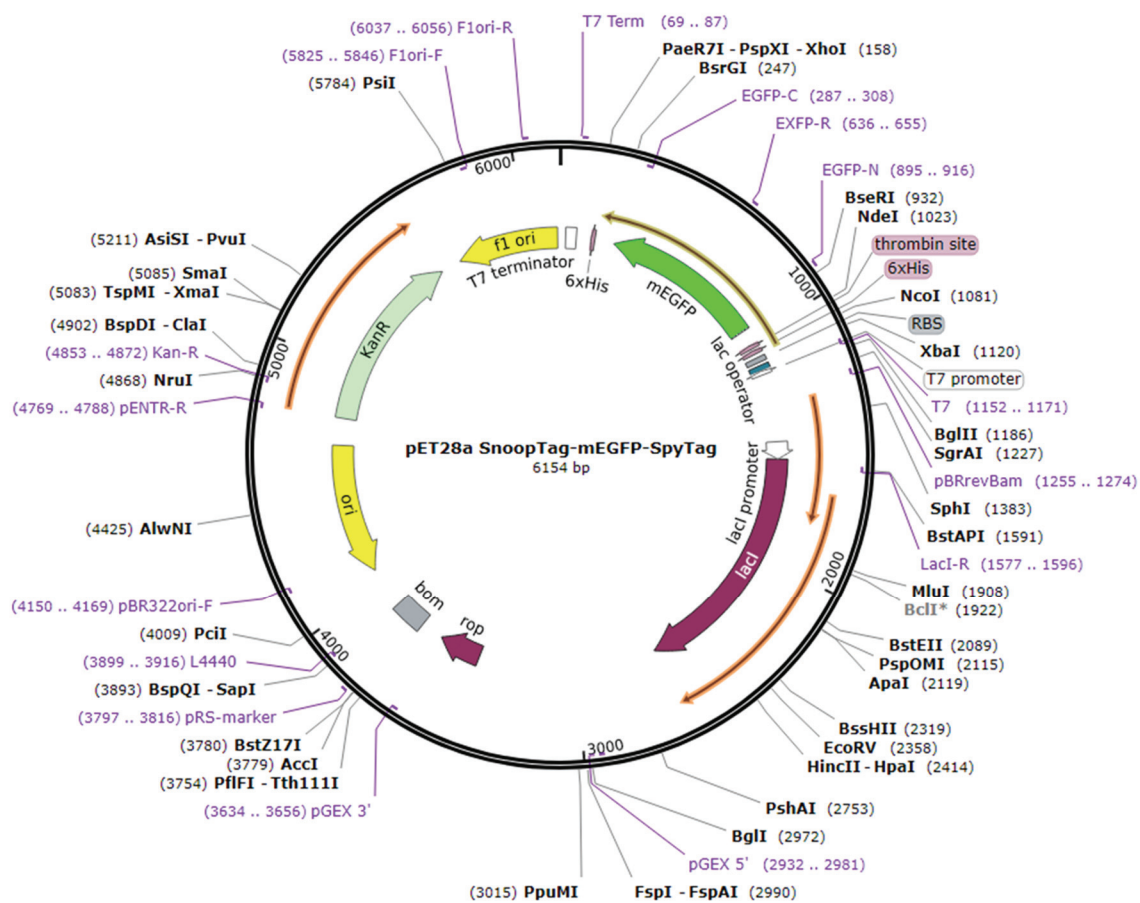
APPENDICES

Appendix A. Plasmid Maps

Created with SnapGene®



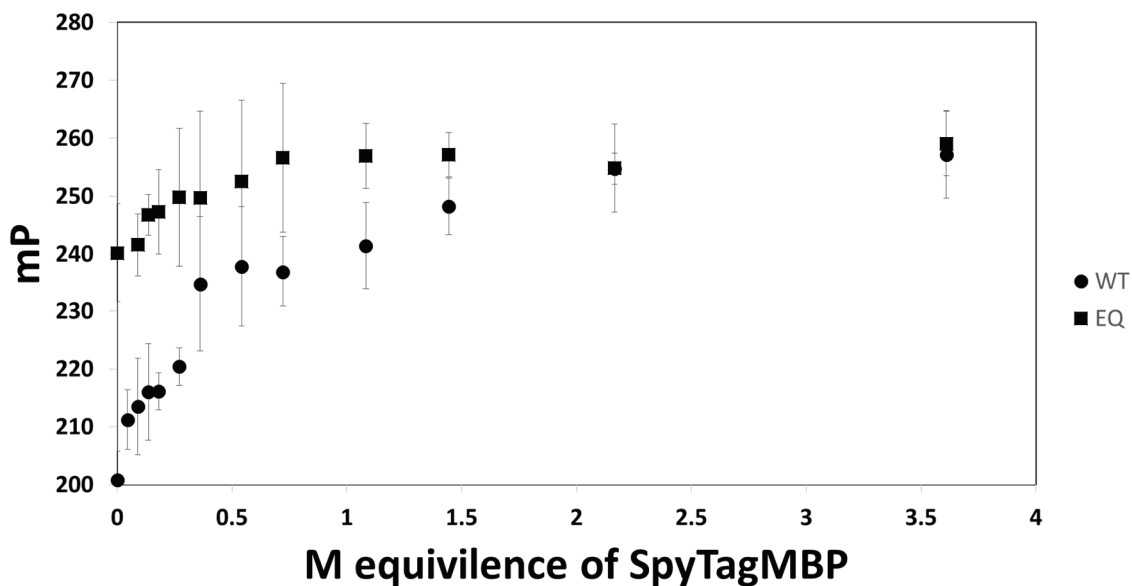
Appendix A-1. pDEST14-SpyCatcher Derivatives. Plasmid map for pDEST14-SpyCatcher and pDEST14-SpyCatcher EQ



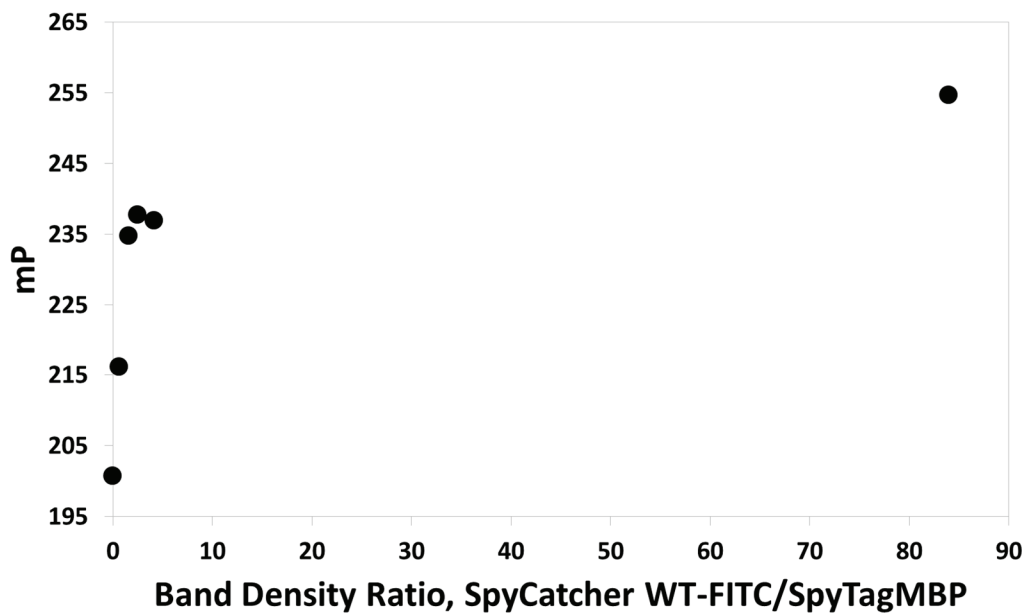
Appendix A-2. pET28a SnooTag-mEGFP-SpyTag. Plasmid map for pET28a.SnooTag-mEGFP-SpyTag.

75

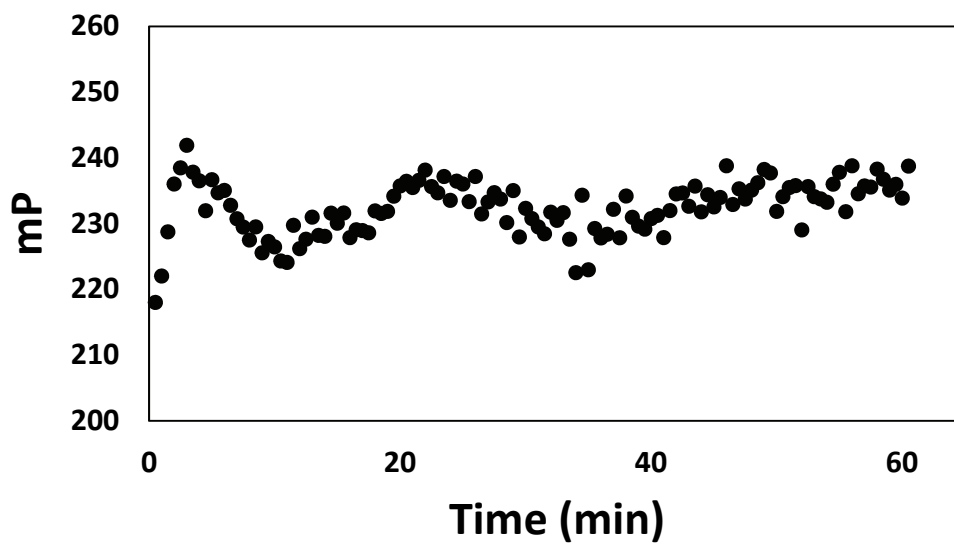
Appendix B. Fluorescence Polarization/Depolarization Graphs



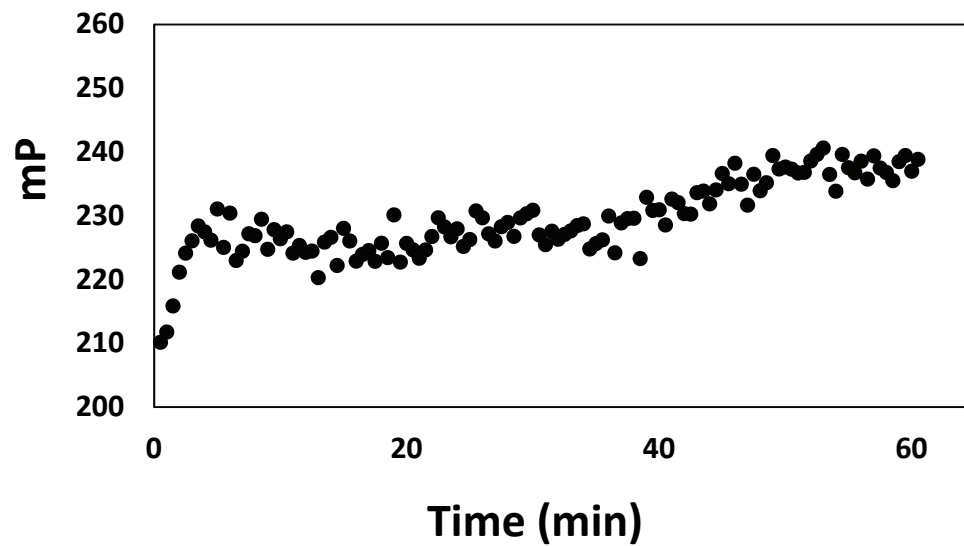
Appendix B-1. Fluorescence Polarization/Depolarization Concentration Dependence. Concentration dependence of fluorescence polarization/depolarization of SpyCatcher WT and SpyCatcher EQ.



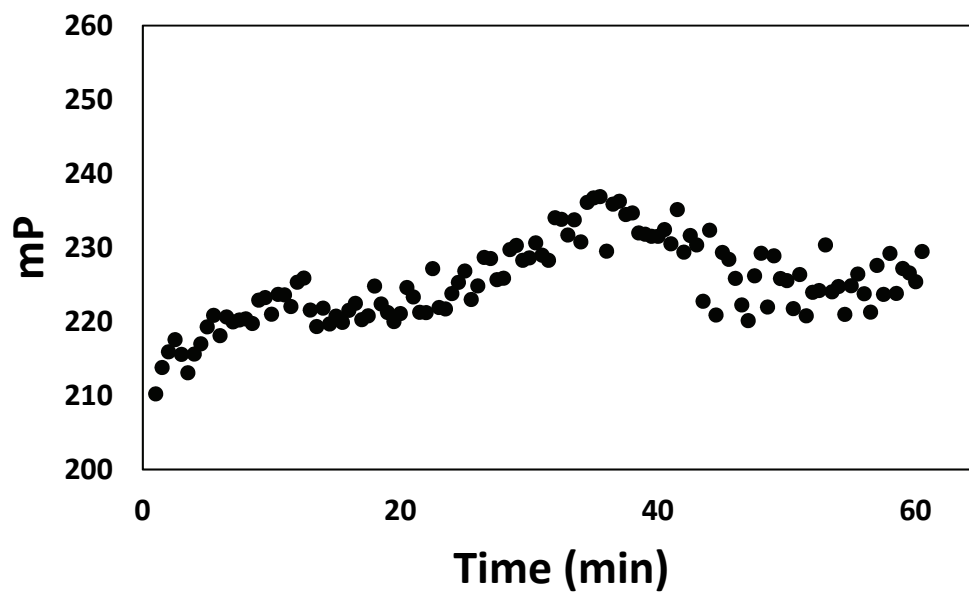
Appendix B-2. Fluorescence Polarization/Depolarization Correlation. Correlation between fluorescence polarization/depolarization measurements with SDS-PAGE band densities



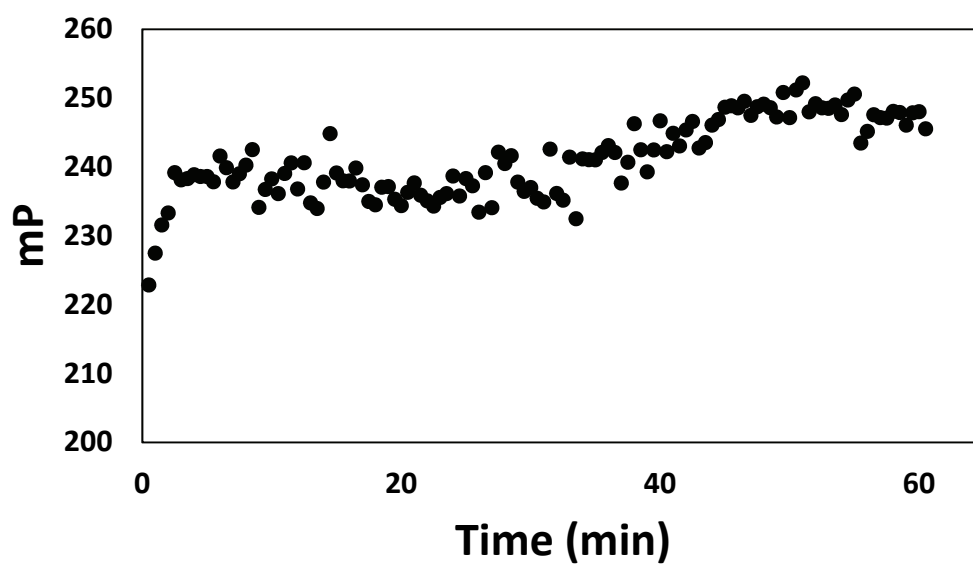
Appendix B-3. Kinetic Run 1.



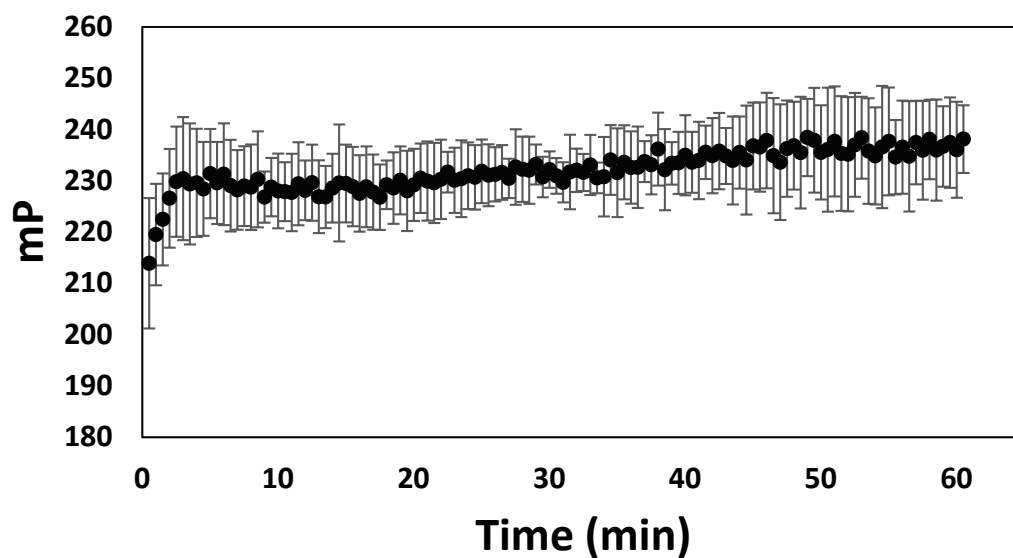
Appendix B-4. Kinetic Run 2.



Appendix B-5. Kinetic Run 3.



Appendix B-6. Kinetic Run 4.



Appendix B-7.Kinetic Study average of four runs with plus or minus one standard deviation error bars.

Appendix C. Molar Equivalence on SDS-PAGE Using ImageJ. Band determined through ImageJ of SDS-PAGE band in **Figure 35**.

M Equivalence of SpyTagMBP	SpyCatcher WT-FITC Band Density	SpyTagMBP-SpyCatcher WT- FITC Complex Band Density
2.166	620	52085
0.722	9379	38834
0.542	12856	31410
0.361	15592	24657
0.181	20309	11919
0	22496	0